

University of Montana

ScholarWorks at University of Montana

Graduate Student Theses, Dissertations, &
Professional Papers

Graduate School

1981

Nature of eastern Montana's climate 1900-1980

Robert A. Boldi

The University of Montana

Follow this and additional works at: <https://scholarworks.umt.edu/etd>

Let us know how access to this document benefits you.

Recommended Citation

Boldi, Robert A., "Nature of eastern Montana's climate 1900-1980" (1981). *Graduate Student Theses, Dissertations, & Professional Papers*. 7355.

<https://scholarworks.umt.edu/etd/7355>

This Thesis is brought to you for free and open access by the Graduate School at ScholarWorks at University of Montana. It has been accepted for inclusion in Graduate Student Theses, Dissertations, & Professional Papers by an authorized administrator of ScholarWorks at University of Montana. For more information, please contact scholarworks@mso.umt.edu.

COPYRIGHT ACT OF 1976

THIS IS AN UNPUBLISHED MANUSCRIPT IN WHICH COPYRIGHT SUBSISTS. ANY FURTHER REPRINTING OF ITS CONTENTS MUST BE APPROVED BY THE AUTHOR.

MANSFIELD LIBRARY
UNIVERSITY OF MONTANA
DATE: 1981

THE NATURE OF EASTERN MONTANA'S CLIMATE, 1900-1980

By

Robert A. Boldi

B.S., Boston College, 1974

**Presented in partial fulfillment of the
requirements for the degree of**

Master of Science

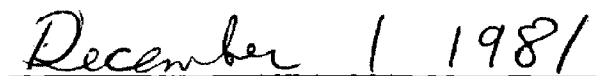
UNIVERSITY OF MONTANA

1981

Approved by:


Chairman, Board of Examiners


Dean, Graduate School


Date

UMI Number: EP38156

All rights reserved

INFORMATION TO ALL USERS

The quality of this reproduction is dependent upon the quality of the copy submitted.

In the unlikely event that the author did not send a complete manuscript and there are missing pages, these will be noted. Also, if material had to be removed, a note will indicate the deletion.



UMI EP38156

Published by ProQuest LLC (2013). Copyright in the Dissertation held by the Author.

Microform Edition © ProQuest LLC.

All rights reserved. This work is protected against
unauthorized copying under Title 17, United States Code



ProQuest LLC.
789 East Eisenhower Parkway
P.O. Box 1346
Ann Arbor, MI 48106 - 1346

ABSTRACT

Boldi, Robert A., M.S., December, 1981

Environmental Studies

The Nature of Eastern Montana's Climate, 1900-1980

Director: R. E. Erickson *RE*

National energy policy presently calls for increased coal mining in the Northern Powder River Basin of eastern Montana. The Montana Strip and Underground Mine Reclamation Act requires that the soils disturbed by this mining be reclaimed. Successful reclamation is defined to be the permanent reestablishment of vegetation upon these disturbed soils.

The Northern Powder River Basin is a semiarid grassland prairie and the availability of moisture is the most critical factor in the successful reestablishment of ground cover. This study characterizes the precipitation patterns of the Northern Powder River Basin in an effort to delimit the types of climates that reclamation activities must tolerate.

The median total spring precipitation is 4 inches with an expected range of 2 to 9 inches within a 20 year period. Rains between 0.10 inch and 1 inch account for 70 percent of this total with 15 percent of the total falling in rains less than 0.10 inch and 15 percent falling in rains greater than 1 inch.

Rain fall occurs on 1 day in 3 with 4.5 days being the median number of days between rains of 0.10 inches or more. The amount of precipitation occurring during any particular time period is very variable as droughts are a common feature of this region. Twice a year, on the average, periods of a month or more pass without any precipitation occurring greater than 0.10 inches. Once every 15 years over 90 days can be expected to pass without any precipitation of this magnitude occurring.

The climate demonstrates long term cyclic variations in the amount of total monthly precipitation with recurrence intervals of 3, 5, and 21 years. The amount of variation represented by each of these long term cycles is about 20 percent of the annual variation in the monthly precipitation levels.

It was concluded that the time period required to demonstrate successful reclamation is on the order of 25 years or more. Given that only five years is presently required to demonstrate to the State that reclamation is successful, changes in the bonding system are suggested.

TABLE OF CONTENTS

	Page
ABSTRACT	ii
LIST OF TABLES	vi
LIST OF FIGURES	vii
Chapter	
1. INTRODUCTION	1
History and purpose of study	1
Data chosen for study	1
Analytical methods chosen	3
Nature of results and conclusions	5
2. LITERATURE REVIEW	7
Causes of climatic change	7
Changes over geologic time	7
Changes over human time	9
Measurement of climatic change	13
Calculating statistical significances	14
Analytical determinations	14
Empirical estimations	15
3. ANALYTICAL METHODS	17
The Fourier transform	17
Mathematical definitions	17
Examples of Fourier transforms	18
Interpretative limits to the Fourier transform	23

Chapter	Page
Correlograms	26
Mathematical definitions	26
Examples of correlograms	28
Importance of correlograms	29
Monte-Carlo simulation technique	32
Necessity of technique	32
Example of technique	34
4. EXPERIMENTAL PROCEDURE	38
Data chosen for study	38
Preliminary statistical analysis	39
Creation of time series	40
Fourier analysis of time series	42
Coherence analysis of time series	43
Construction of the average annual correlogram	43
Significance of average correlogram	45
Accuracy of Monte Carlo simulations	46
Analysis of expected future precipitation levels	47
5. RESULTS	48
Summaries of seasonal and annual precipitation	48
Summary of the number of days between rains	53
Time series analysis	56
Coherence analysis	64

Chapter	Page
6. DISCUSSION	66
Limitations of the data base	66
Mathematical procedures	66
Climatological analysis	67
LITERATURE CITED	72
APPENDICES	
A. DERIVATION OF CONFIDENCE LIMITS FOR THE VALUE OF PI	76
B. TABLES OF RAW DATA	78
Seasonal Data	78
Billings	78
Busby	80
Crow Agency	82
Miles City	84
Average monthly total precipitation	86
C. GENERATION AND TESTING OF RANDOM NUMBERS	87
The generation of random deviates	87
FORTRAN program to produce random numbers	90
The testing of RANDU'S random numbers	91
First 100 random numbers used	95
D. FORTRAN program to calculate the fast Fourier transform	96

LIST OF TABLES

Table	Page
1. Statistical Summary of the Total Seasonal and Annual Precipitation of All Weather Stations and All Years of Record	48
2. Percent of Days Having at Least Indicated Amounts of Precipitation	52
3. Percent of Total Precipitation from Rains of at Least Indicated Size	52
4. Number of Times per Year that a Specified Number of Days Will Pass Without Various Amounts of Precipitation	55

LIST OF FIGURES

Figure	Page
1. Location of Northern Powder River Basin and weather stations utilized in study (Billings, Busby, Crow Agency, and Miles City)	2
2. Various representations of $Y = \text{SINE}(2\pi X/5)$	19
3. Various representations of $Y = 0.67\text{SINE}(2\pi X/5) + 0.33\text{SINE}(2\pi X/20)$	19
4. Various representations of $Y = 0.5\text{SINE}(2\pi X/5) + 0.5\text{SINE}(2\pi X/20)$	20
5. Various representations of $Y = 0.33\text{SINE}(2\pi X/5) + 0.67\text{SINE}(2\pi X/20)$	20
6. Various representations of $Y = \text{SINE}(2\pi X/20)$	22
7. Various representations of $Y = \text{SINE}(2\pi X/5) * \text{SINE}(2\pi X/20)$	24
8. Various representations of $Y = \text{SINE}(2\pi X/5) * \text{SINE}(2\pi X/40)$	24
9. Correlogram of random series	30
10. Correlogram of Markoff series, $p=0.10$	30
11. Correlogram of Markoff series, $p=0.25$	30
12. Fourier transform of Markoff series, showing the increase in expected amplitudes with increasing correlation of consecutive terms and increasing period . .	31
13. Target at which darts are thrown to determine the numerical value of Pi	35
14. Randu's approximation to Pi as well as the distribution of expected results as a function of total trials	37
15. Correlation of average mean annual temperature and average mean annual precipitation for all weather stations and all years of record	41

Figure	Page
16. Relationships between temperature, precipitation and P/E indices for Billings and Miles City, 1950-1976	41
17. Histograms of total seasonal precipitation at all weather stations and all years of record	50
18. Histogram of total annual precipitation at all weather stations and all years of record	51
19. Percent of days with at least a given amount of precipitation and the percent of the total annual precipitation due to these events	54
20. Percent of dry spells exceeding various lengths of time . .	57
21. Historical records of seasonal precipitation	58
22. Average Fourier transform of region with various confidence limits	60
23. Distributions of the maximum amplitude of a random average Fourier transform	63
24. Average annual correlogram of region with confidence levels	65

Chapter 1

INTRODUCTION

History and purpose of study

The Montana Strip and Underground Mine Reclamation Act requires that surface soils disturbed by mining be reclaimed. In defining successful reclamation, the Act requires that the vegetation growing upon a disturbed site be capable of regenerating itself under the natural conditions prevailing at that site. The conditions prevailing in an area must be thought of as that area's long term climatological characteristics, for its recent climate may well be a historical anomaly. The time scale on which to characterize the climate should be commensurate with the characteristic time scale of mine reclamation activities, i.e. weeks to decades.

The Northern Powder River Basin of eastern Montana (Figure 1) has been targeted for increased coal production over the next few decades. Consequently, a description of its climate is needed in order to be able both to delimit the range of expected climates and to specify the implications inherent therein for stripmine reclamation activities.

Data chosen for study

Of the many climatic variables (temperature, hours of sunlight, wind mileage, or snow cover etc.), precipitation most strongly influences the vegetative growth in the semi arid Great Plains and is often the limiting growth factor (U.S.G.S., 1979). Because of this

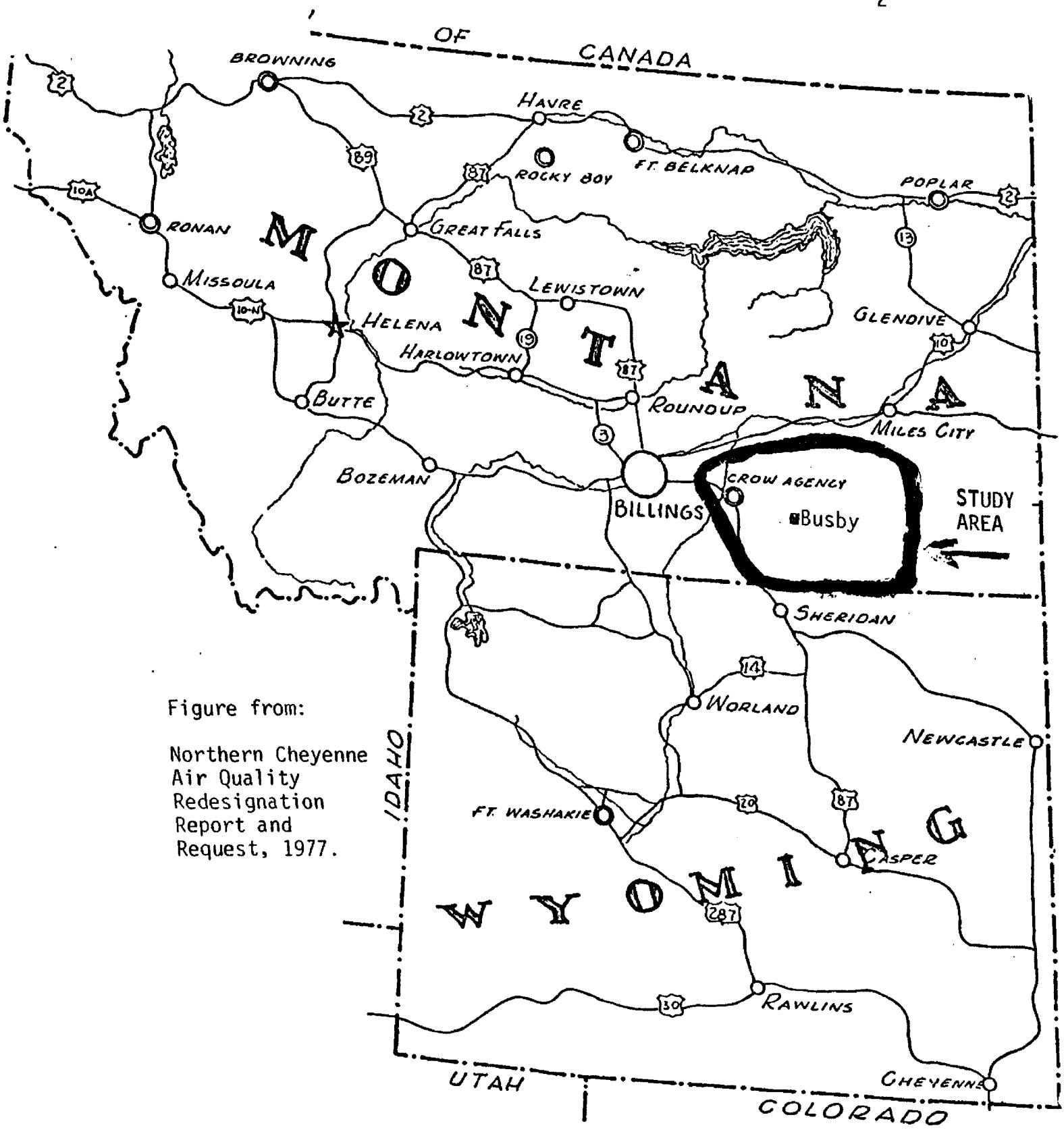


Figure from:
Northern Cheyenne
Air Quality
Redesignation
Report and
Request, 1977.

Figure 1. Location of Northern Powder River Basin and weather stations utilized in study (Billings, Busby, Crow Agency and Mules City).

biological (and agricultural) significance of moisture, precipitation was chosen as the basic element of study.

Precipitation is measured over time intervals ranging from minutes to years, and different phenomenon are affected by the amounts of precipitation falling during characteristic time intervals. For example, hydraulic erosion of soils is caused by high instantaneous rain fall rates while the overall climate of a region can be conveniently described by the average monthly total precipitation.

The length of time between rains is also important to reclamation activities in as much as wind erosion of soils results from long dry spells in areas without adequate cover of drought resistant vegetation.

To describe the average climatological characteristics existing over a large area, long term weather records from many locations must be utilized.

This paper examines, therefore, the precipitation history of the Northern Powder River Basin as indicated by the four eastern Montana weather stations for which unbroken records exist back to at least 1911 (Billings, Busby, Crow Agency, and Miles City).

Analytical methods chosen

Two distinct lines of analysis were carried out in order to characterize the nature of the precipitation in this region. The first was a statistical summary of the daily, monthly, seasonal and annual precipitation levels as well as a summary of the expected number of days between rains of various sizes. Considering the date on which a

particular observation was made permits the detection of any long term changes in these variables. If these variations can be ascribed to some physical, causal mechanism, then the future precipitation patterns of the area might be predictable. This type of analysis is often called time series analysis.

Time series analysis began with the calculation of the average Fourier transform of the region's monthly precipitation record. To accomplish this, each weather station's monthly precipitation record was first normalized and its discrete Fourier transform computed. The corresponding Fourier amplitudes from each transform were then averaged to produce the average Fourier transform of the region's monthly precipitation record.

Each amplitude in this average Fourier transform represents the relative contribution to the monthly precipitation levels from a periodic variation of a particular cycle time (i.e. wave length). The statistical significances of these average amplitudes were tested by empirically determining the distributions of the average amplitudes if no long term, periodic variation is present via the Monte-Carlo simulation technique. This technique was used in order to avoid the extensive mathematical analysis required to analytically determine the distributions of the average Fourier transform under the chosen null hypothesis.

To complement this Fourier analysis, the correlogram of each series was computed and the corresponding autocorrelation coefficients from each correlogram averaged. The significances of these average autocorrelation coefficients were also determined via the Monte-Carlo

simulation technique.

This average correlogram was then compared with the correlograms of time series having different generating functions in an effort to further elucidate the nature of the precipitation patterns of the region. This average correlogram allows the discrimination between Markoff, cyclic and random processes; an important distinction when discussing the physical forces thought to be influential in determining the precipitation levels at any given time.

Nature of conclusions drawn

Based on the statistical analyses of the precipitation levels observed at the weather stations in the area, the 20 year minimum and maximum expected seasonal and annual precipitation levels were determined as well as the frequencies of occurrence of rains of various sizes and their relative contributions to the total rainfall. The distributions of the number of days between rains of various sizes were also determined. These climatic parameters serve to delimit the types of conditions that reclamation activities must tolerate.

Based on the time series analyses of these same weather records, the time scale of climatic variations was determined. Given that reclaimed land must be permanently revegetated, and that permanency implies the ability to withstand all normal climatic conditions, these analyses suggested the minimum time needed to assure successful reclamation. This length of time was compared with the length of time presently considered adequate to demonstrate successful reclamation and policy recommendations were subsequently made.

Based on the ease with which the statistical tests utilized in these time series analyses were performed, the Monte-Carlo technique was shown to be applicable to studies of this type and extends the range of climatic studies that can be performed without resort to intractable mathematical manipulations.

Chapter 2

LITERATURE REVIEW

Causes of climatic change

Changes over geologic time. Since the Earth's formation some 4.5 billion years ago, it has undergone evolutionary changes in both its physical form and biological constituency. Because the various climates of the past have played a major part in this process, performing the physical act of weathering the Earth's surface and providing the physical boundary conditions for developing biological life, studies of climatic changes are being carried out by many different disciplines, each with its own temporal and spatial scales of interest.

The field of paleoclimatology deals with the climatic changes that have occurred over the past four billion years and consequently a review of its recent advances will serve to place the question of more recent climatic changes into perspective. Measurable forces known to operate over long time scales that can have an effect upon the climate are those associated with the movements of the continents over the surface of the Earth and the variations in the Earth's orbital parameters.

The first of these forces, plate tectonics, is a powerful agent of climatic change due to its rearrangement of the continental blocks' latitude and longitude and the accompanying changes in the global oceanic and atmospheric circulation patterns (Pearson, 1978). These changes

occur over periods of time measured in tens to hundreds of millions of years and they can consequently be considered to redefine the overall physical climatic state of the Earth within which other factors operate to produce smaller, shorter term, variations.

The climatic changes introduced as a result of the movement of the continental blocks can be rapid however, as the opening and closing of seaways, known to have profound impacts upon the climate of the world, can be rapid (Flohn, 1979). In fact, evidence that drastic, rapid climatic changes are the norm is found in such diverse records as Grand Pile peat bogs (Woillard, 1978) and the Camp Century, Greenland ice cores (Johnson et al., 1975).

Periodic variations in the Earth's orbital parameters and their effect upon the climate have been under intensive study since Milankovitch popularized the theory in 1941. In this theory, the periodic variations in the degree of eccentricity of the Earth's elliptical orbit around the Sun (varying between 0.014 and 0.05 with a periodicity of 93,000 years), the precession of the major axis of the Earth's orbit (making a 360 degree revolution every 21,000 years) and changes in the angle between the Earth's equatorial axis and the plane of the ecliptic (varying between 22 and 25 degrees with a periodicity of 41,000 years) combine to produce variations in both the total solar radiation received by the Earth and its seasonal and latitudinal distribution (Kukla, 1975).

The amount of this variation has been calculated by Berger (1978) for the past million years while Weertman (1976) and Schneider & Thompson (1979) have predicted the effects that these variations should

have upon the climate and have found them to be of sufficient magnitude to produce the known sequence of periodic ice ages. Hays et al. (1976) summarize the physical evidence linking the ice ages to these orbital variations and find that "changes in the Earth's orbital geometry are the fundamental cause of the succession of Quaternary ice ages."

Recently, the discovery of an anomalously high level of iridium at the boundary of the Cretaceous and Tertiary epochs (about 65 million years ago) has given rise to the theory that periodic impacts of asteroids 10 ± 4 Kilometers in diameter may precipitate dramatic climatic changes (Smit and Hertogen, 1980) and cause wide spread extinctions and adaptations (Alvarez et al. 1980; Hsu, 1980).

Changes over human time. Turning now to climatic changes measured in centuries and decades rather than eons and millennia, three forces thought to effect the climate have been suggested. These are variations in the solar output, vulcanism, and human activities.

Studies of a wide range of climatic variables; the incidence of forest fires (Vines, 1977a), North American temperature records (Mock and Hibble, 1976), Midwest drought indicators (Roberts and Olson, 1975), dendrochronological data (Douglass, 1919), sea surface temperature records (Loder and Garrett, 1978), and isotopic oxygen ratios (Hibler and Johnsen, 1979) have revealed periodic variations of approximately 20 years. This commonality has lead to a search for a common cause.

In as much as the sun is known to undergo periodic changes in sunspot activity with a recurrence interval of about 20 years, attempts have been made to postulate a mechanism linking sunspot variations with

variations in the Earth's climate. At first the total solar luminosity was thought to be modulated with this periodicity, with the maximum during the sunspot minimum and vice versa (Abbot, 1976). More recent satellite studies have revealed however, (White, 1977) that there is no such variation in the solar constant.

Measurements of the solar flux during the sunspot maximum of 1969 and the minimum of 1976 indicate that there is less than 1 percent variation in the solar constant over the sunspot cycle. This amount of variation can be put into perspective by noting that there is a 7 percent variation in the solar constant due to the seasonal changes in the Earth-Sun distance. A persistent 1 percent change in the annual solar radiance is estimated to change the average global surface temperature by 0.5 degrees Kelvin to 5 degrees Kelvin.

Markson (1978) has shown however, that variations in the levels of ionizing radiation reaching the Earth's ionosphere can produce variations in world wide storm activity and it is known that the amount of ionizing radiation reaching the Earth does vary by many orders of magnitude over the solar cycle (White, 1977).

Measurements made in the soft X-ray region (100 to 10 Angstroms) indicate a 5 to 100 fold variation in solar luminosity over the sun spot cycle. Measurements in the hard X-ray region (10 to 1 Angstroms) reveal variation from 100 to 1000 fold over the solar cycle. Variation in the flux of these X-rays has great importance in terrestrial atmospheric physics as they are the primary ionizers of the ionosphere. Changes in the rate of ionospheric ionization will produce world wide changes in the global electric field, a parameter known to interact with the

thunderstorm network; although it is not now possible to predict, a priori, what the net effect would be of a world wide increase in the Earth's electric field (Dicke, 1979).

The long term existence of the presently observed regular variation in sunspot activity is in question moreover, as the lack of sun spots for many years was noted in the 1700's and is referred to as the Maunder minimum (Eddy, 1976).

Volcanic dust veils have been proposed as a cause of climatic change because they scatter and absorb incoming solar radiation thereby cooling the lower atmosphere (the troposphere) and warming the upper atmosphere (the stratosphere). Schneider and Mass (1975) have taken the historical record of dust veil indices as compiled by Lamb (1970) and compared the predicted effects of volcanic dust in the atmosphere with historical climatic data and have concluded that volcanos can effect the global climate to a significant degree. Similar calculations were carried out by Hansen et al. (1978) and the predicted atmospheric temperature changes were in excellent agreement with the observed temperature changes resulting from the Mount Agung eruption of 1963. In the troposphere, these changes amounted to a cooling of 0.5 degrees Celsius, an amount known to have global consequences.

Bray (1974) has shown the synchronicity of periods of intense volcanic activity and periods of global glaciation. Periods of intense volcanic activity are not randomly distributed with time more ever (Lamb, 1970; Hirschboeck, 1980), but are a result of periodically changing solar and lunar forces which combine to produce periods of maximum probability for volcanic eruptions once every 19 years.

All of the above mentioned causes of climatic change are deterministic in nature, that is, they are viewed as variables external to the Earth which, through some physical mechanism linking the two, cause the Earth's climate to respond in some predictable way. Some workers (i.e. Hasselmann, 1976; Lorenz, 1970, 1968) have pointed out that the climatic changes over time could just as well be described as internal oscillations of the climate caused by the interactions of the various earthly components of the climatic system, without regard to changes in any external variables (orbital parameters, sunspots, etc.).

Perhaps one of the more controversial of the proposed causes of climatic change is human activities, especially in the areas of energy production and land disturbances. Anthropogenic production of carbon dioxide (Manabe and Wetherald, 1975), and Fluorochlorocarbons (Rowland and Molina, 1975), as well as changes in the earth's albedo caused by desertification (Charney, 1975) have the ability to influence the climate, tending to cause a global warming.

Results of attempts to calculate the magnitude of the expected effects are highly speculative however, given the essentially unquantifiable interactions of the various components of the climatic system. It is known however, that there are many self reinforcing feedback mechanisms present, so small changes in the climate can be self propagating (Hecht et al., 1979). Consequently, humanity's ability to influence the climate, in theory at least, is undisputed.

Whether or not any of the recently observed climatic changes can be ascribed to human activities is speculative at present, with some workers claiming an effect (i.e. Budyko, 1977a, 1977b) and others

holding the opposite opinion (i.e. Bryson, 1974).

Measurement of climatic change

Just as there are many different theories as to what causes climatic change, so too there are many different approaches to measuring climatic change. The climatic indicator chosen to study in a particular project is normally dictated by the temporal and spatial scales on which one wishes to work, while the particular method of statistical analysis chosen is determined by the computing resources available and the nature of the data at hand.

Prior to the advent of the modern high speed computer, optical methods were often used to search for periodicities and the statistical significances of any observed periods were, quite literally 'eyeballed' (Douglass, 1919). With the computer came the ability to perform almost limitless numerical computations and the field of time series analysis opened up.

In time series analysis, there are two main statistical tests used, harmonic analysis and coherence analysis. Harmonic analysis is the application of the Fourier transform to a time series to test for the presence of regular, periodic variations in the data. Examples of studies using this technique are Hibler and Johnsen, 1979 and Vines, 1977a, 1977b.

Coherence analysis is the investigation of the correlation between two different functions (or a function and itself) at different amounts of relative offset. Examples of studies using this technique are Frankignoul and Hasselmann, 1976 and Kominz & Pisiyas, 1979.

Estimating statistical significances

Analytical determinations. With either of these two procedures, if the null hypothesis is that the data are a realization of Gaussian noise, or a Markoff process of some specified order, then the distribution of the test statistics (the amplitudes of the Fourier transformation and the autocorrelation coefficients of the correlogram) can be determined analytically (see for example Frankignoul and Hasselmann, 1976; Kominz and Pisiyas, 1979). If the null hypothesis is complicated in some way then the test statistic used must have its distribution under the null hypothesis determined. Unfortunately, it is all too easy to generate a null hypothesis for which the distribution of the test statistic either has not or can not be determined analytically.

This can happen either by performing some operation upon the data whose effect upon the distribution of test statistics is unknown, or if the assumptions of the null hypothesis are violated in any way. For example, the most commonly violated assumption is that of the data being normally distributed. In these cases the test statistic must have its distribution determined either analytically or empirically (Conover, 1971). This has limited the statistical analyses of multiple stations in many works. For example, Bradely (1976), in his extensive analysis of the early precipitation history of the Rocky Mountain states, counted the number of statistically significant results in a set of 100 stations. If there were around 5 significant results at the 0.05 probability level, then their overall significance was placed in doubt.

In the climatic studies referred to earlier in this section, in each case, the null hypothesis was a simple one, namely that the data is a single realization of either Gaussian noise or a Markoff process of some specified order. If multiple stations are to be analyzed, then the stations are usually individually summarized and the geographical distribution of means (for different time periods) are plotted as isopleths (for example Diaz and Quayle, 1980; Walsh and Mostek, 1980).

In principle, the Fisher randomization method can be used to determine the distribution of any test statistic. Consequently any null hypothesis, no matter how complicated, can be tested (Conover, 1971). Unfortunately the Fisher method involves the enumeration of each and every possible permutation of the data and the generation of the test statistic for each permutation and then determining where the test statistic obtained from the actual data under test falls in the distribution of all possible test statistics. This could easily take years of computer time if the number of possible outcomes is large and hence only a subset of all possible combinations can be tested. This brings into play the technique known as Monte-Carlo simulation.

Empirical estimations. In this process random numbers are used to generate representative null data sets from which the distribution of the required test statistic can be calculated. Using the Monte-Carlo method to generate as many different null data sets as required, and from them generating the distribution of the proposed test statistic, the probability of obtaining the observed test statistic by chance alone can be easily determined. This obviates the need for modifying the null

hypothesis to allow use of a statistical test for which the distribution of test statistics is already worked out or analytically determinable (Newman and Odell, 1971).

Chapter 3

ANALYTICAL METHODS

The Fourier Transform

Mathematical definitions. Essentially the Fourier transform decomposes a series of numbers into a large number of sine waves of different frequencies. These sine waves, when added back together again, reproduce the original series. By measuring the amplitude of each resulting sine wave, one can estimate its relative contribution to the original series. The larger any one sine wave's amplitude is relative to all the others, the more strongly the original data resembles that particular sine wave. Mathematically, the discrete Fourier transform can be stated as:

$$H(f)_k = \sum_{j=0}^{n-1} [X(t)_j e^{2\pi i f t_j} dt] \quad \text{for } k=0,1,2,\dots,(n/2)$$

Because $H(f)_k$ is a complex number, it can be represented as:

$$H(f)_k = R(f)_k + i I(f)_k = |H(f)_k| e^{i\theta(f)_k}$$

Where:

$$R(f)_k = \text{the real part of } H(f)_k$$

$$I(f)_k = \text{the imaginary part of } H(f)_k$$

$$|H(f)_k| = \sqrt{R(f)_k^2 + I(f)_k^2} = \text{the Fourier amplitude}$$

and

$$\theta(f)_k = \tan^{-1} [I(f)_k / R(f)_k] = \text{the phase of sine wave relative to the origin}$$

The values of $R(f)_k$ and $I(f)_k$ were found via the so called

fast Fourier transformation introduced by Cooley and Tukey (1965). To see how the Fourier transform works in practice, some sine waves of various wavelengths and their corresponding Fourier transforms are now presented.

Examples of the Fourier transform. Figure 2a is a sine wave with a wave length of 5 units and an amplitude of 1 unit of arbitrary measure. For the purposes of this study, the amplitude (Y axis) can be considered to be the precipitation levels at any given time and the X axis can be considered to be the time of observation (in years). Figure 2a can therefore be thought of as a precipitation record displaying a periodicity of 5 years. Figure 2b is its corresponding Fourier transform. Notice the single peak located at 5 years in the transform. This indicates that there is but a single sine wave in Figure 2a with a wave length of 5 years. Figures 3, 4, and 5 superimpose increasing amounts of a 20 year sine wave on the original 5 year sine wave.

In Figure 3a, the composition is 1/3 times the 20 year sine wave plus 2/3 times the 5 year sine wave. In this figure, the sum of the two most strongly resembles the 5 year sine wave, but the 20 year sine wave

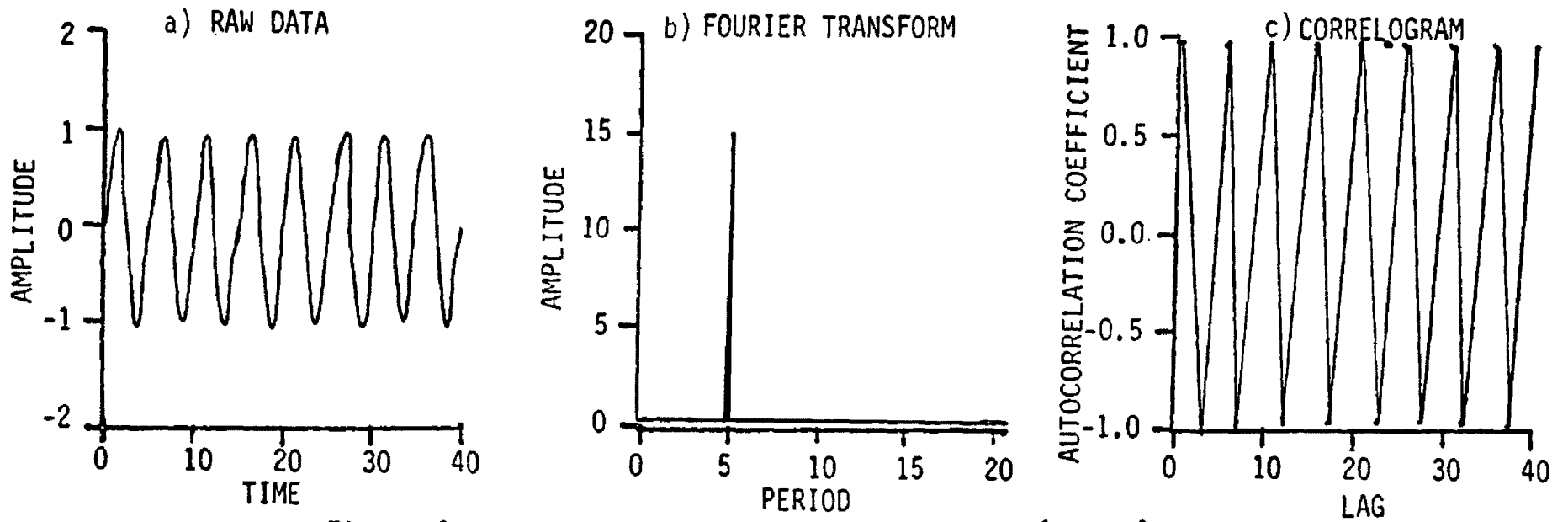


Figure 2. Various representations of $Y = \sin(2\pi t/5)$.

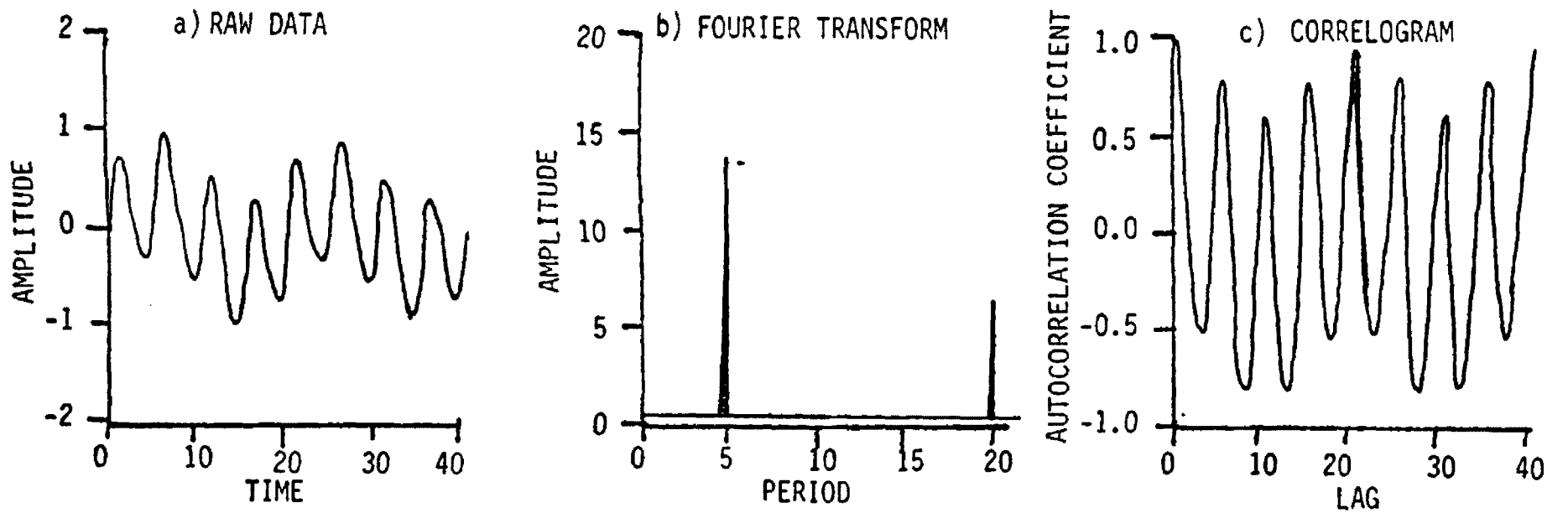


Figure 3. Various representations of $Y = \frac{2}{3}\sin(2\pi t/5) + \frac{1}{3}\sin(2\pi t/20)$.

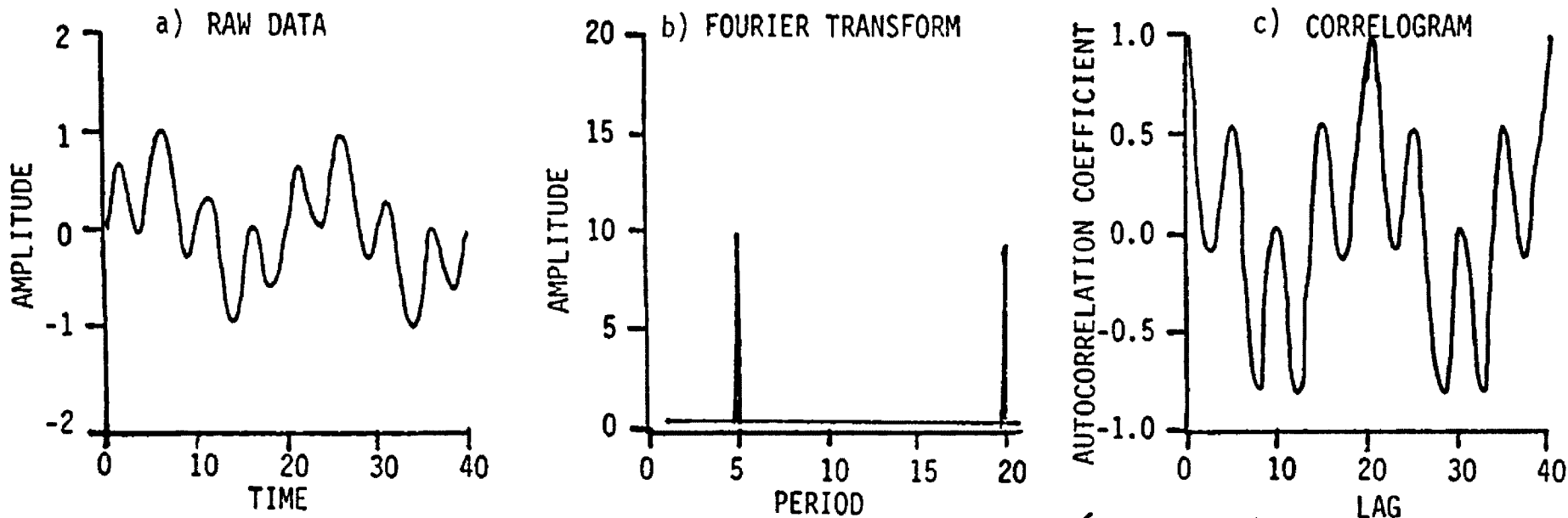


Figure 4. Various representations of $Y = \frac{1}{2} \sin(2\pi x/5) + \frac{1}{2} \sin(2\pi x/20)$

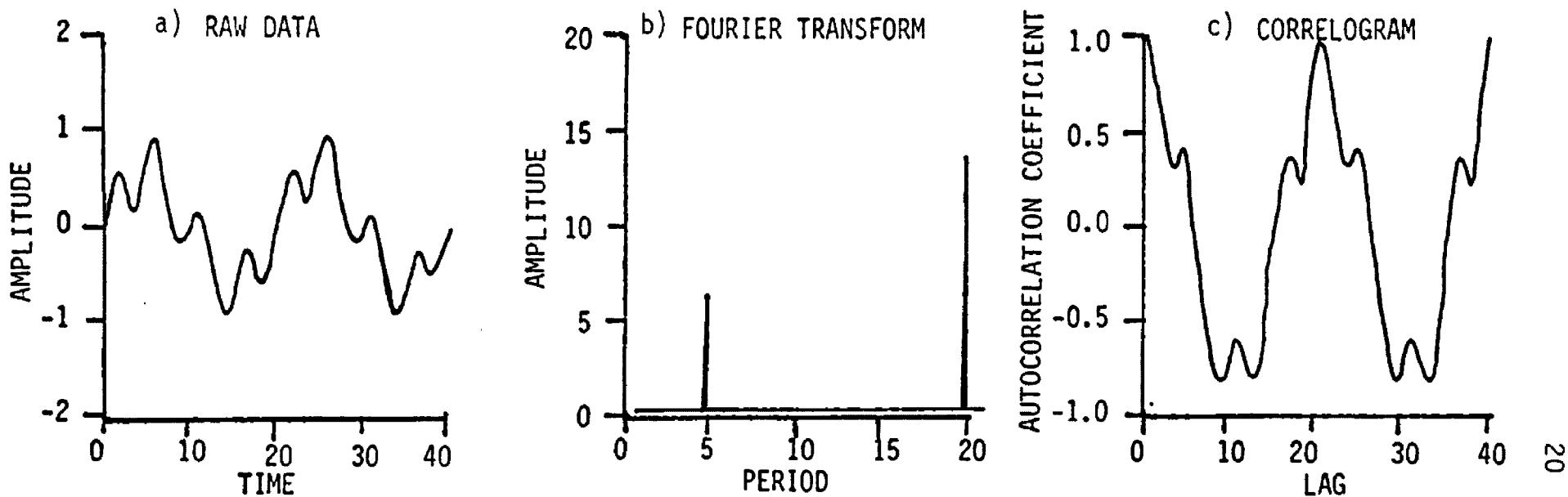


Figure 5. Various representations of $Y = \frac{1}{3} \sin(2\pi x/5) + \frac{2}{3} \sin(2\pi x/20)$

can be seen to be present also. This longer wavelength sine wave manifests itself by the gentle rise and fall of the consecutive peaks of the dominant 5 year sine wave. Turning to Figure 3b, the Fourier transform of Figure 3a, the peak at 5 years is seen to be larger than the peak at 20 years by just the ratio of the weights given to the individual sine waves in constructing the composite series shown in Figure 3a, namely 2:1.

Figure 4a was constructed by adding together equal parts of each of the two sine waves, and this results in the two peaks in the Fourier transform (Figure 4b) being equal.

Turning to Figure 5a, the sum of $\frac{2}{3}$ times the 20 year sine wave plus $\frac{1}{3}$ times the 5 year sine wave, it is seen that this figure most strongly resembles a pure 20 year sine wave with smaller 5 year sine wave peaks superimposed upon it. This impression is born out by Figure 5b which is the Fourier transform of Figure 5a. Here the peak at 20 years is seen to dominate the 5 year peak and the ratio of the two is just the ratio of the weights given to the two sine waves in making up Figure 5a; i.e. 2:1.

Turning finally to Figures 6a, a pure sine wave of 20 years, and 6b, its Fourier transform, a single peak at 20 years is seen in the Fourier transform, indicating that there is but a single sine wave present in Figure 6a and its wavelength is 20 years.

The salient point here is that both the relative strengths and frequencies of the component sine waves can be determined from the Fourier transform of the composite series.

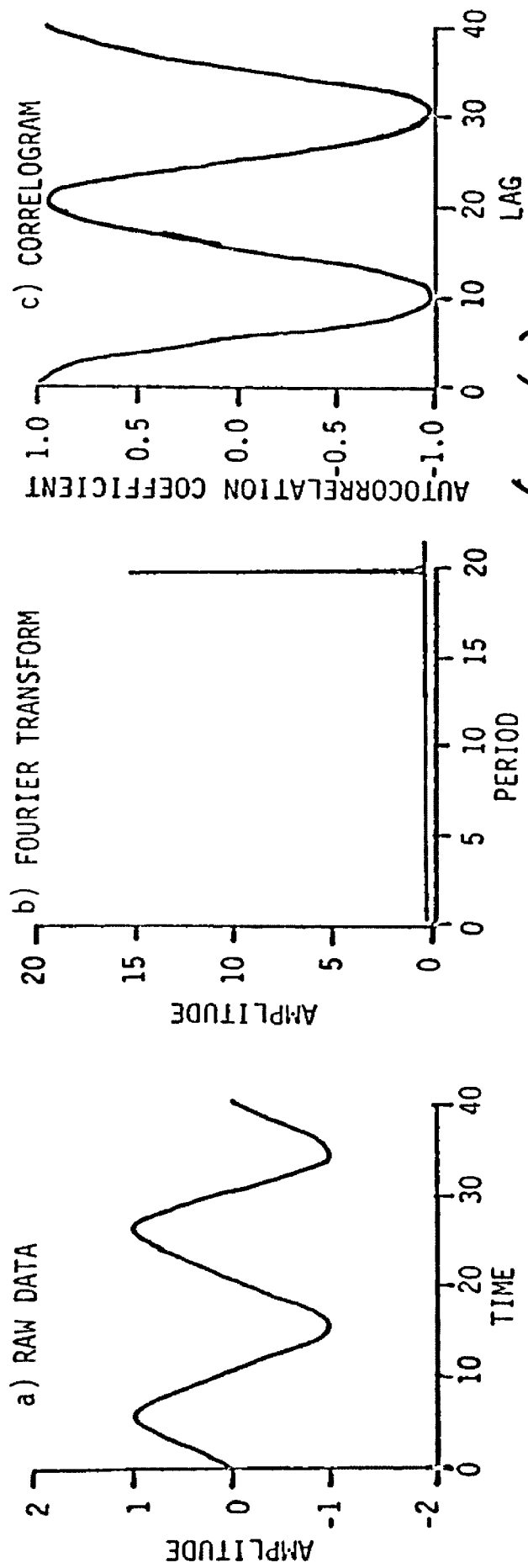


Figure 6 . Various representations of $Y = \sin(2\pi x/20)$

Interpretative limits to the Fourier transform. Due to the particular manner in which the two sine waves were combined in the above examples, i.e. by addition, the peaks in the Fourier transforms of the sum of the two series are in the same places that they occupied in the Fourier transforms of the individual sine waves. This additive property is summarized by the following equation:

$$\text{Fourier transform}(X+Y) = \text{transform}(X) + \text{transform}(Y)$$

If a different way of combining the two sine waves is used, however, then there is no assurance that individual peaks found in the Fourier transform arise from individual, component sine waves of an equal wavelength present in the original data.

For example, if the two sine waves used in the above examples are multiplied together, then the resulting Fourier transform will have no peak at the longer sine wave's frequency, (frequency being the reciprocal of wavelength, i.e. $1/20 = .05$), and the peak at the shorter sine wave's frequency (i.e. $1/5 = .2$) will be split into two peaks, centered at the frequency of the shorter sine wave and separated by the frequency of the longer sine wave. In other words, there are two peaks seen in the spectrum, located at $0.2 \pm .05$ reciprocal years (or 4.0 and 6.7 years).

This is shown in Figures 7a and 7b. Figure 7a is a time series constructed by multiplying together the 5 year sine wave and the 20 year sine wave and its Fourier transform is shown in Figure 7b.

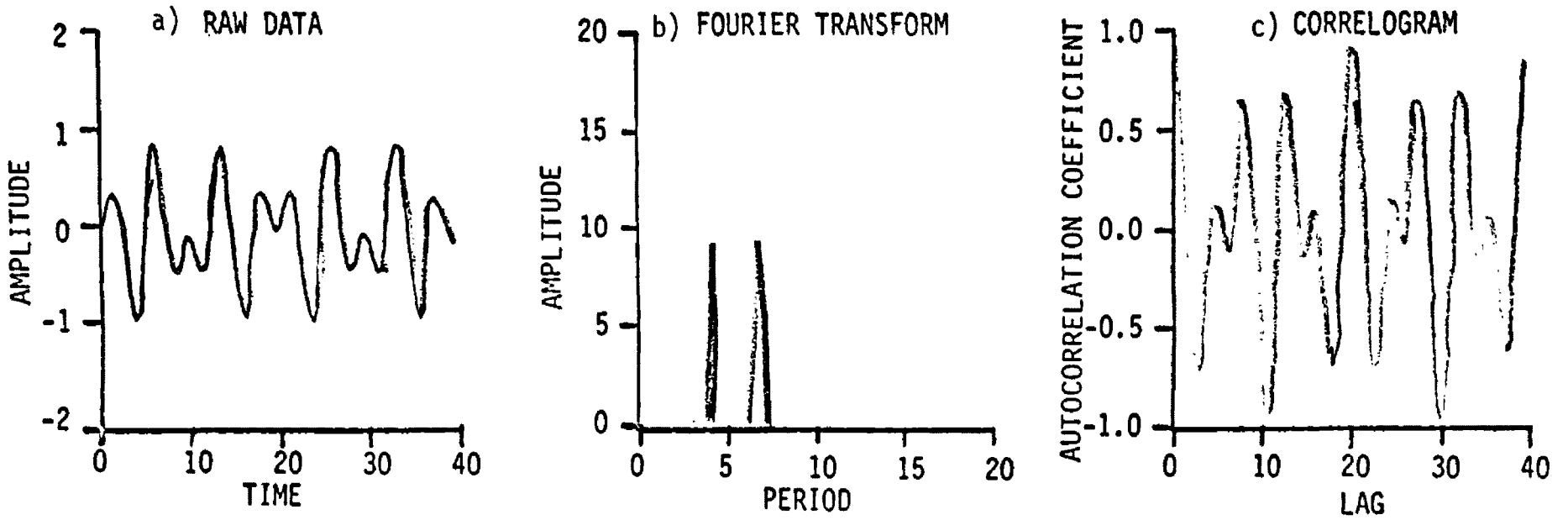


Figure 7 . Various representations of $Y = \text{SIN}(2\pi X/5) * \text{SIN}(2\pi X/20)$

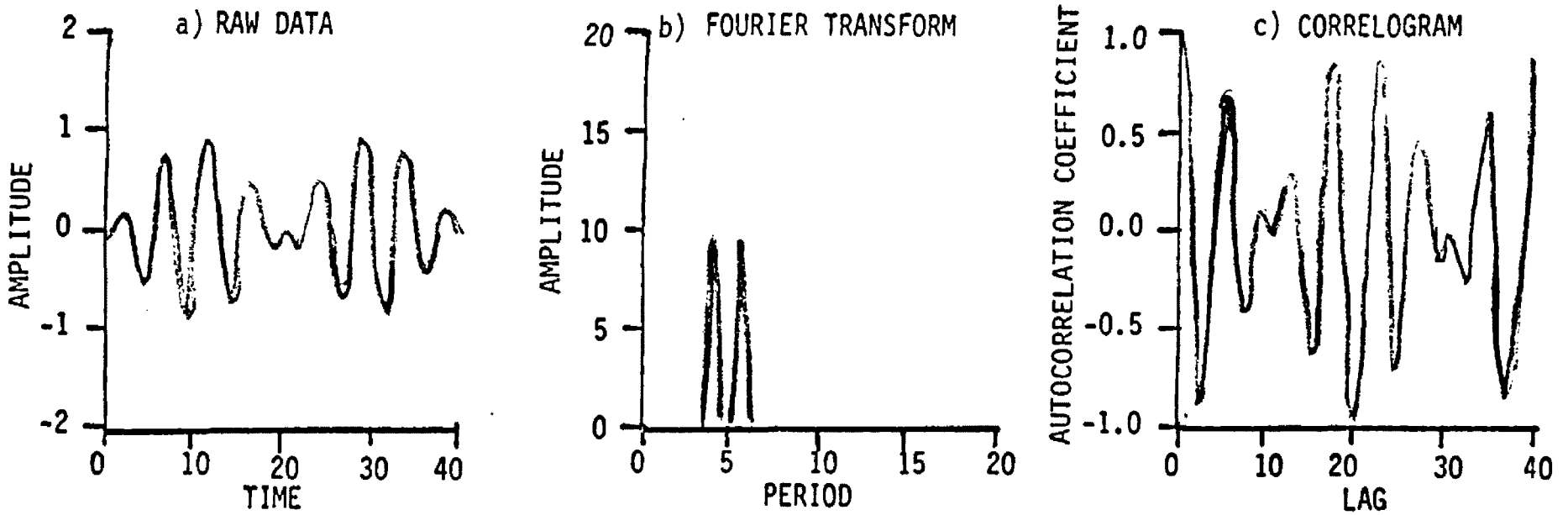


Figure 8 . Various representations of $Y = \text{SIN}(2\pi X/5) * \text{SIN}(2\pi X/40)$

This demonstrates the point that if a sinusoidal time series is the simple sum of a number of contributing sine waves, then the location of the peaks in the Fourier transform of the resultant series can be thought of as the periods of the contributing, or component, sine waves. If a more complicated interaction is hypothesised, however, then the Fourier Transformation of the interacting sine waves must be analytically (or empirically) determined.

The Earth's climatic system is known to have many components that can interact with each other. Some of these interactions result in feedback mechanisms of a self propagating nature. For example, a warming trend would cause some ice in the polar regions to melt, thereby reducing the average albedo. This in turn causes more heating and this in turn causes more ice melting (Gribbin, 1978).

These facts indicate that there may be no simple, additive model of the climate that would allow the individual peaks in a Fourier transform of some climatic variable to be unequivocally assigned to discrete components of the climatic system with characteristic periodicities equal to the frequencies of the peaks seen in the Fourier transform.

This is especially true of interacting climatic components having similar response times, for as the difference between the periods of the interacting sine waves grows larger, this peak splitting feature of a multiplicative interaction becomes less noticeable. In other words, as the wavelength of the longer sine wave increases, relative to the shorter sine wave, its frequency decreases, and the shorter period's peaks are not split as badly. This is demonstrated in Figures 8a and 8b

(shown on page 24). In Figure 8a, the 5 year sine wave is multiplied by a 40 year sine wave (twice the wavelength as used in Figure 7a and 7b), while Figure 8b shows that the distance between the doublet representing the 5 year sine wave is halved relative to Figure 7b and is now located at $.2 \pm 0.025$ reciprocal years (or 4.44 and 5.71 years).

Correlograms

Mathematical definitions. The correlation between the two variables

X and Y is defined to be $r_{X,Y}$ which is equal to:

$$r_{X,Y} = \frac{\text{STD}_{X,Y}}{\text{STD}_X * \text{STD}_Y} = \frac{\sum_{i=1}^n [X(i)*Y(i) - \bar{X}\bar{Y}]^2}{\sqrt{\sum_{i=1}^n [X(i) - \bar{X}]^2 * \sum_{i=1}^n [Y(i) - \bar{Y}]^2}}$$

An autocorrelation coefficient is a measure of the correlation between terms of a series separated by a specified number of terms. The amount of separation between terms being correlated is the called the lag. This procedure can be understood by analogy to the product moment correlation coefficient defined above.

To calculate the autocorrelation coefficient at a given lag (r_j), we replace the pair of variables (X_i, Y_i) with the pair (X_i, X_{i+j}) where j is the lag at which the autocorrelation coefficient is calculated. For a random series, the

expected value of r_j , symbolized by $E(r_j)$, is given by:

$$E(r_j) = \frac{-1}{n-1} = 0 \text{ for large } n$$

The variance is given by:

$$\text{Var}(r_j) = \frac{(n-2)^2}{(n-3)^3} = \frac{-1}{n} \text{ for large } n$$

If, on the other hand, persistence is present, then a Markoff process can be said to be operating. In this process, the autocorrelation coefficient at lag 1 is a measure of the dependence that a given term has upon the preceding term. If each term influences only the succeeding term, then a first order Markoff process is operating and the series can be described as:

$$X_{t+1} = X_t * p + E$$

Where

E is a random deviate

p is the correlation between successive terms

The expected value of r_j can be expressed as:

$$E(r_j) = p^j - \left[\frac{1-p}{n-j} - \frac{1+p}{1-p} (1-p)^j + 2jp^j \right]$$

In practice, p is estimated by the autocorrelation coefficient at lag 1 [$r(1)=p$].

The autocorrelation coefficient is seen above to vanish as j increases for a first order Markoff process. If, however, the time series is truly cyclic, with period L and phase θ , i.e. :

$$X_t = p \cdot \text{sine}\left[\frac{t}{L}(-2\pi) + \theta\right] + E$$

then, as will be shown below, $E(r_j)$ will not vanish as j increases,

but will itself be periodic with the same period as the original series.

By comparing the average correlogram produced from the four stations' time series with the correlograms from random, cyclic, and Markoff processes, we can determine which of these three processes is occurring. Representative correlograms of each of these three types of processes are now presented.

Examples of correlograms. Turning first to the cyclic process discussed earlier (Figures 2 thru 6), a striking resemblance is seen between a cyclic time series (Figures 2a thru 6a) and its corresponding correlogram (Figures 2c thru 6c). The main point to note here is that for a cyclic series, the autocorrelations do not vanish with increasing lag but are themselves cyclic with the same period as the original series.

Figure 9 shows the distribution of the autocorrelation coefficients as a function of lag for a random series. It is seen that all the lags have a mean value of approximately 0 as stated earlier.

Turning next to the correlograms of two Markoff series, one with $p = 0.1$ (Figure 10) and the other with a $p = 0.25$ (Figure 11), it can be seen that the expected value of p decreases as p raised to the j power as mentioned earlier. The confidence limits in Figures 9 thru 11 can be seen to widen as the lag increases. This is due to the fact that the number of pairs of values that can be formed in any given series decreases with increasing lag and the variance of the expected autocorrelation coefficient increases with decreasing number of pairs of terms.

Figure 12 shows that the effect that a Markoff process has upon the Fourier transform of a time series. The expected value of the Fourier amplitude is seen to increase with increasing period length for a given Markoff correlation and an increase in the Markoff correlation is seen to increase the expected values of all the amplitudes. This is an example of the so called 'red noise' phenomenon.

Importance of correlograms. Knowledge of the amplitudes of a Fourier transform is not, in and of itself, sufficient to determine the internal structure of a time series. This is due to the possible presence of persistence in the series. Persistence can be defined here as a tendency for wet months to follow wet months and dry months to follow dry months (due some physical property of the climate) with no cyclic nature involved. This is a Markoff process and if it is occurring, then the Fourier amplitudes of the longer period sine waves will be, on the average, greater than what they would be if this persistence was not present in the series (as shown in Figure 12).

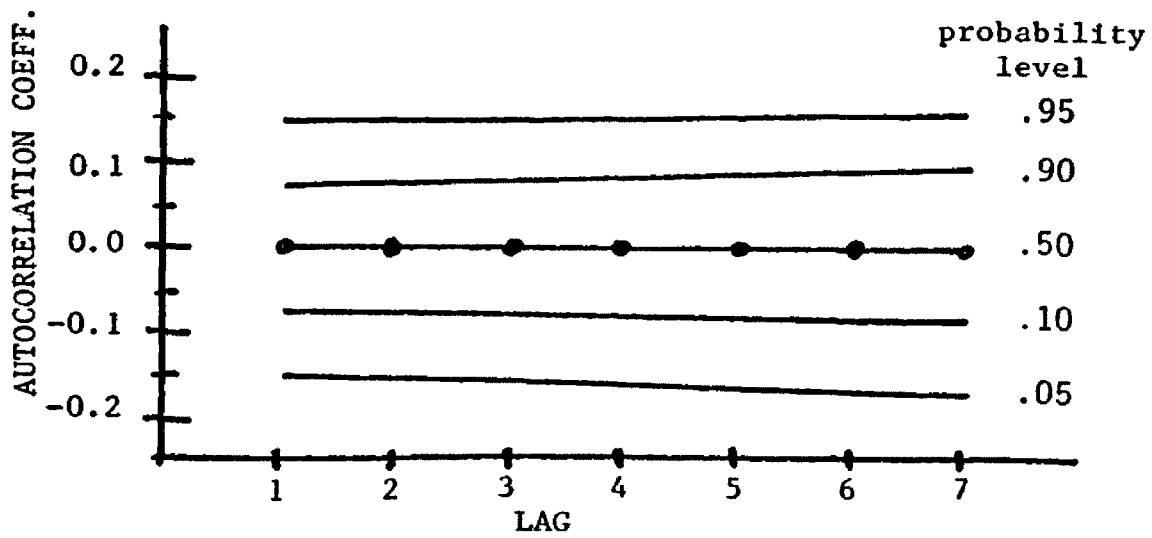


Figure 9. Correlogram of random series.

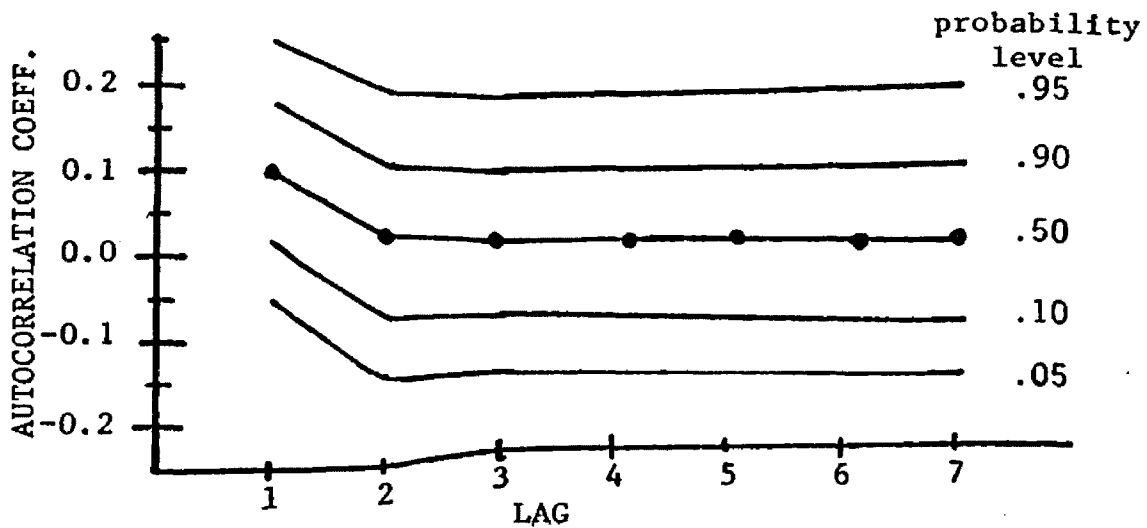


Figure 10. Correlogram of Markoff series; $p=0.10$

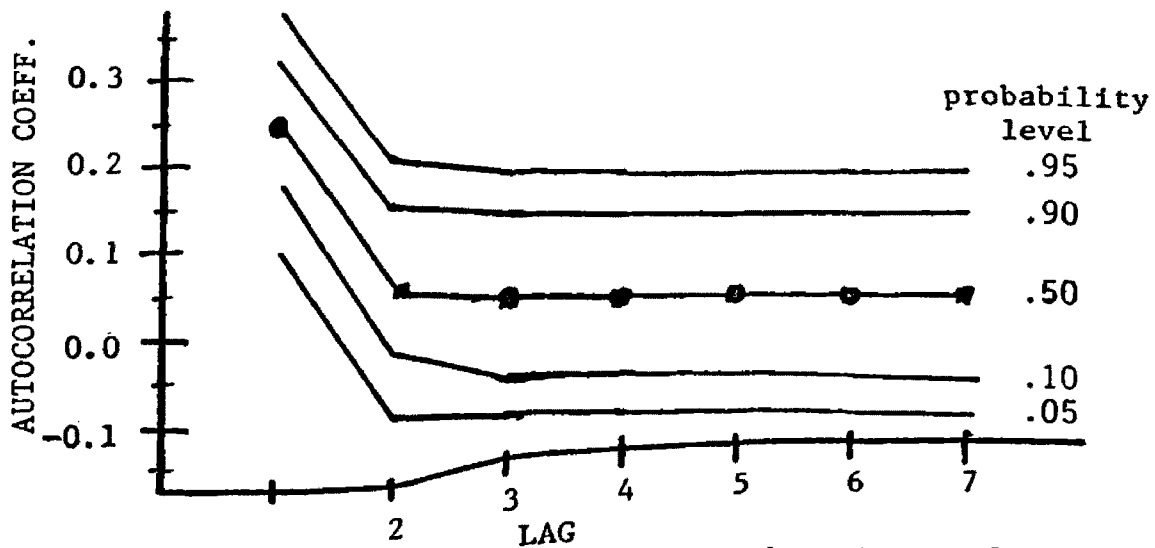


Figure 11. Correlogram of Markoff series; $p=0.25$

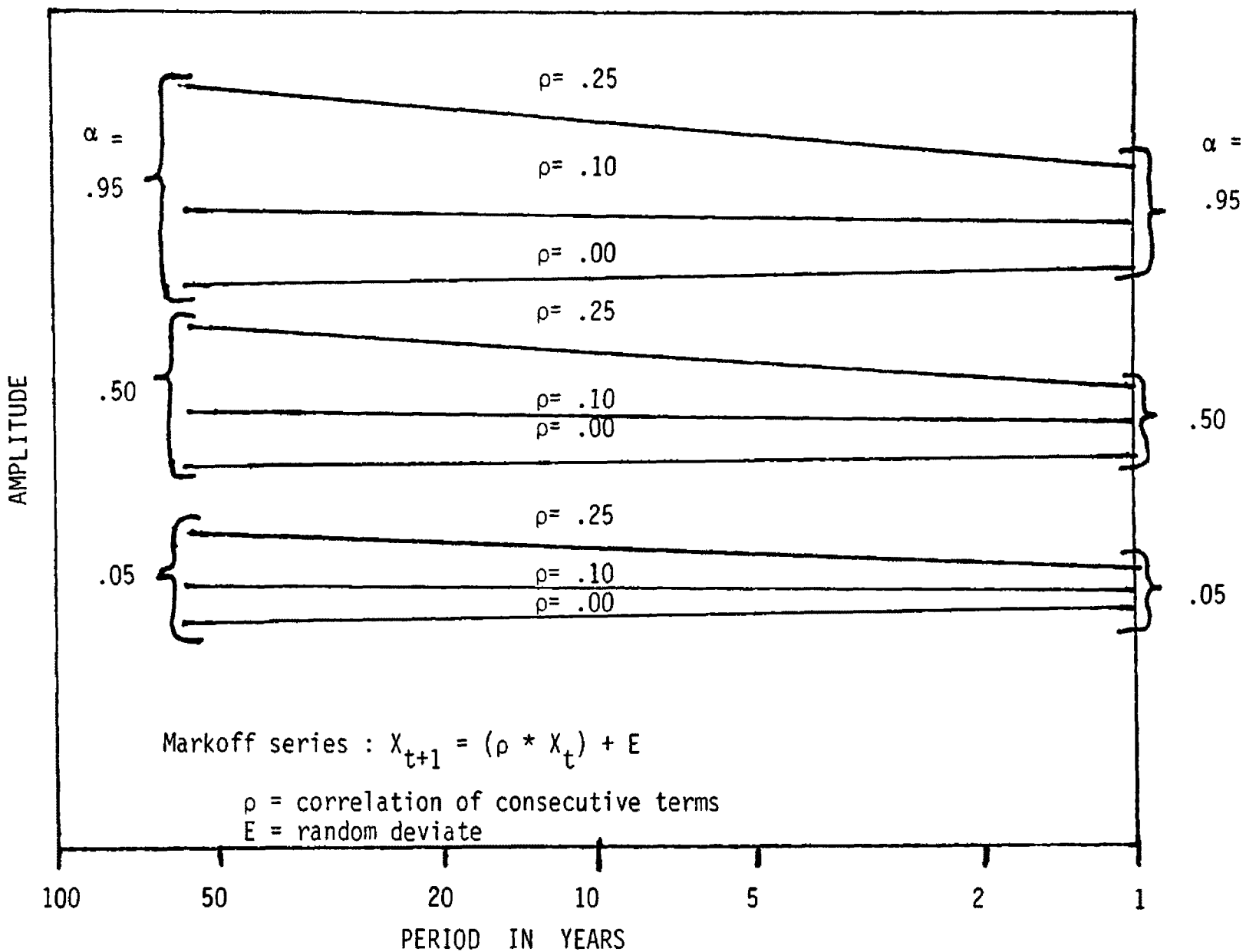


Figure 12. Fourier transform of Markoff series, showing the increase in expected amplitudes with increasing correlation of consecutive terms and increasing period.

This possibility was investigated by calculating the autocorrelation coefficients for various time lags for each historical precipitation record and then averaging the coefficients for corresponding lags. This results in an average autocorrelation coefficient for each lag which can then be plotted against the length of the lag to produce a correlogram, the shape of which can indicate what types of processes can be considered to be generating the time series under study.

As seen in the above examples, if the correlogram displays a high autocorrelation coefficient at small lags and progressively decreases as the lag increases, then a Markoff process can be considered to be operating. If the correlogram is itself cyclic, then a cyclic process can be considered to be operating, and if the correlogram shows random fluctuations, then a random process can be considered to be operating.

The Monte-Carlo simulation technique

Necessity of technique. The data in studies of this type are often transformed into a simple realization of Gaussian noise (or a Markoff process) by summing the rain fall totals over some time interval that represents the longest known period of oscillation (normally 1 year). This was decided against here for four reasons.

First, it was desired to obtain the greatest spectral resolution that was possible. If the data were to be summed into yearly values, then the shortest period that could be resolved would be 2 years. By analyzing the monthly values, periods as short as 2 months could be

resolved.

Second, there was no compelling reason to choose any particular months as comprising a precipitation year. The water year (October thru September), used by hydrologists, reflects the storage of fall precipitation as snow, which is subsequently released in the spring. The calendar year is just as good a candidate, since January is normally one of the drier months, and may minimize any side effects of splitting the year during one of the wetter seasons.

Third, the data was truncated using the Hanning function:

$$x(t) = 0.5*(1.-\cosine(2\pi*t/T))$$

This function is used to reduce the undesirable effects of truncating the time series after a given number of terms (Brigham, 1974). This is an example of performing an operation upon the data whose effect upon the resulting distribution of test statistics is unknown.

Fourth and most importantly, it was desired to relate the magnitude of the longer term variations in the data to the annual variation. This would be impossible to do if the data were first summed into yearly values for there would no longer be any yearly variation to serve as a reference against which to measure the other variations.

All this serves to indicate that the data should not be summed into yearly values. This introduces the known intraannual variation into the null hypothesis, and changes the resulting distribution of the null test statistic. As the annual variation becomes larger and larger, the amount of variation due to the other periods becomes smaller in proportion.

Consequently, I could not analytically derive the null distribution of the amplitudes of the average Fourier transform of the precipitation records of the four stations under consideration. Therefore, I was forced to empirically determine it via the Monte-Carlo simulation technique.

Example of technique. To see how this method can be employed to find the numerical solution to a problem too complex to be solved analytically, the method is used to find the numerical value of Pi.

This can be done by noting that the ratio of the area of the unit circle to the area of the unit square is $\text{Pi}/4$. The unit circle can be inscribed in the unit square, and when it is, it divides the unit square into two subareas. One subarea is all the area outside of the unit circle and the other is all the area inside of the unit circle. This situation is depicted in Figure 13.

Figure 13a can be imagined to be a target at which darts will be thrown at random (uniformly distributed in both the X and Y direction). By counting both the number of darts that land within the unit circle and the total number of darts thrown, the amount of area within the circle relative to the whole area (i.e. the ratio of the area of the circle to the area of the square) can be estimated. This ratio is an approximation to $\text{Pi}/4$, from which an estimate of Pi can be obtained.

This process can be carried out by generating uniformly distributed random numbers between -1 and +1 and pairing them into points (X,Y) and counting how many of all such points fall within the unit circle ($X^2+Y^2<1$). Figure 13b shows one quadrant of this target

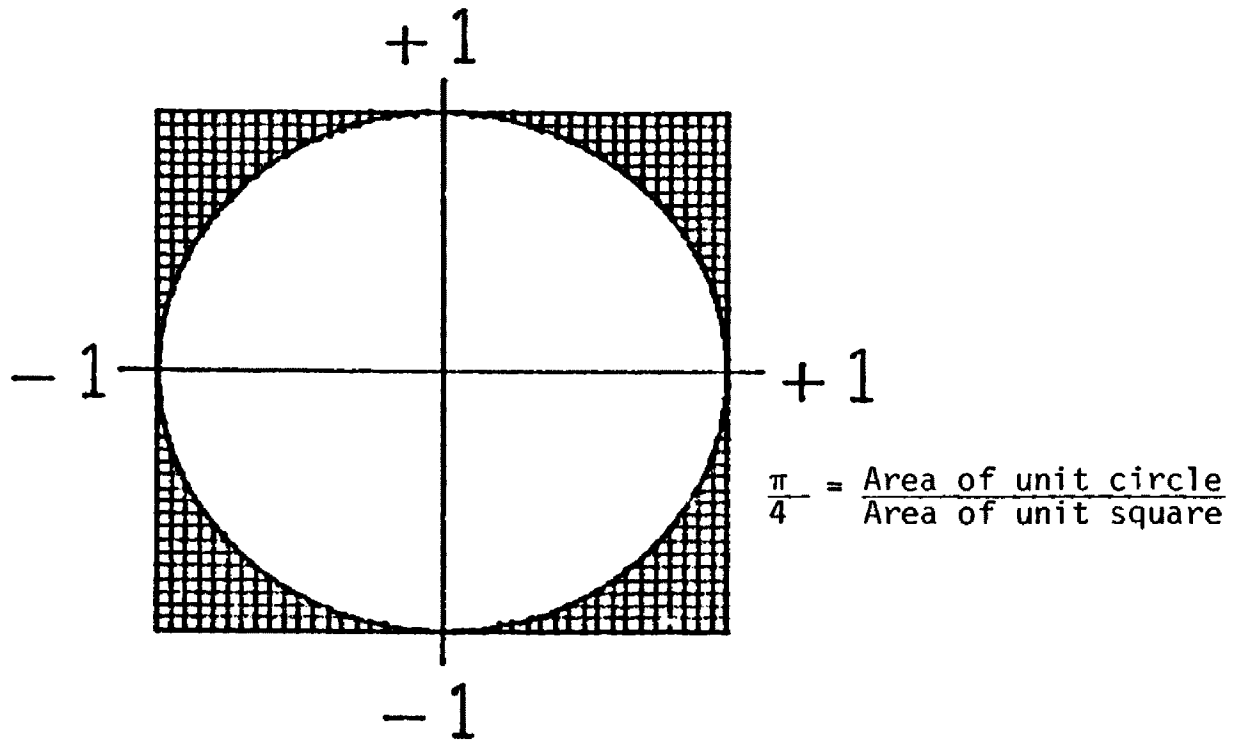


Figure 13a. The unit circle inscribed within the unit square. The area of the unit circle is π and the area of the unit square is 4.

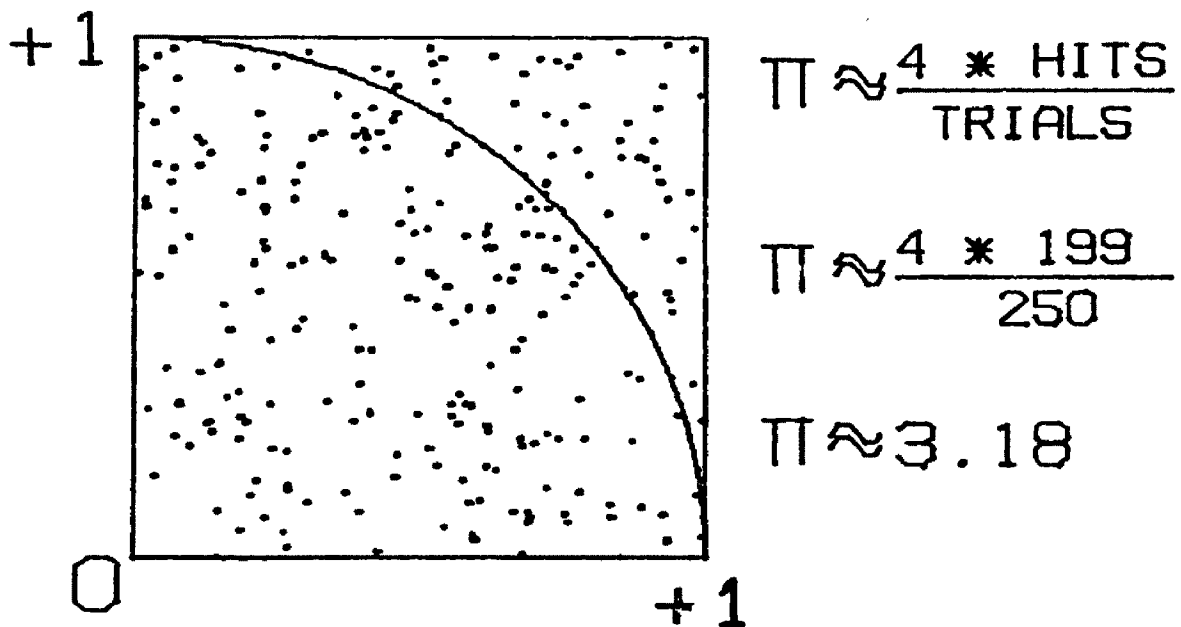


Figure 13b. One quadrant of Figure 13a, at which 250 points are randomly placed in a numerical approximation of π .

at which 250 darts have been thrown, resulting in 199 hits. From this particular trial 3.18 is estimated as the value of Pi.

As the number of trials increases, the ratio of hits (points falling within the circle) to total trials will converge to the ratio of $\text{Pi}/4$. Then, by multiplying the observed ratio by 4, an estimate of Pi is obtained. Figure 14a shows the result of generating 2.5 Million random (X,Y) points, taking the ratio of hits to total tries and multiplying by 4. The value of Pi obtained via this process is 3.1435 which, while not a particularly accurate value, is within 0.1 percent of the true value. If this entire procedure were repeated 1000 times, a more accurate estimation of Pi would (probably) be arrived at.

In this simple example, the probability of any given number of hits out of a given number of total trials can be calculated because in fact, the value of Pi is known already. This has been done to demonstrate to fact that the Monte-Carlo technique estimates, with a finite degree of error, the required statistic; the value of Pi.

Figure 14a shows the predicted distribution of results if such a repetition were to be carried out. The method of determining the probability distribution of expected results is shown in Appendix A.

Figure 14b shows the 0.90 and 0.99 probability level limits to the amount of error expected in the estimation of Pi as a function of the number of trials performed. It can be seen from this figure that any desired degree of precision can be obtained by increasing the number of trials, but due to the probabilistic nature of the procedure itself, the accuracy of any particular outcome can only be known in a statistical sense.

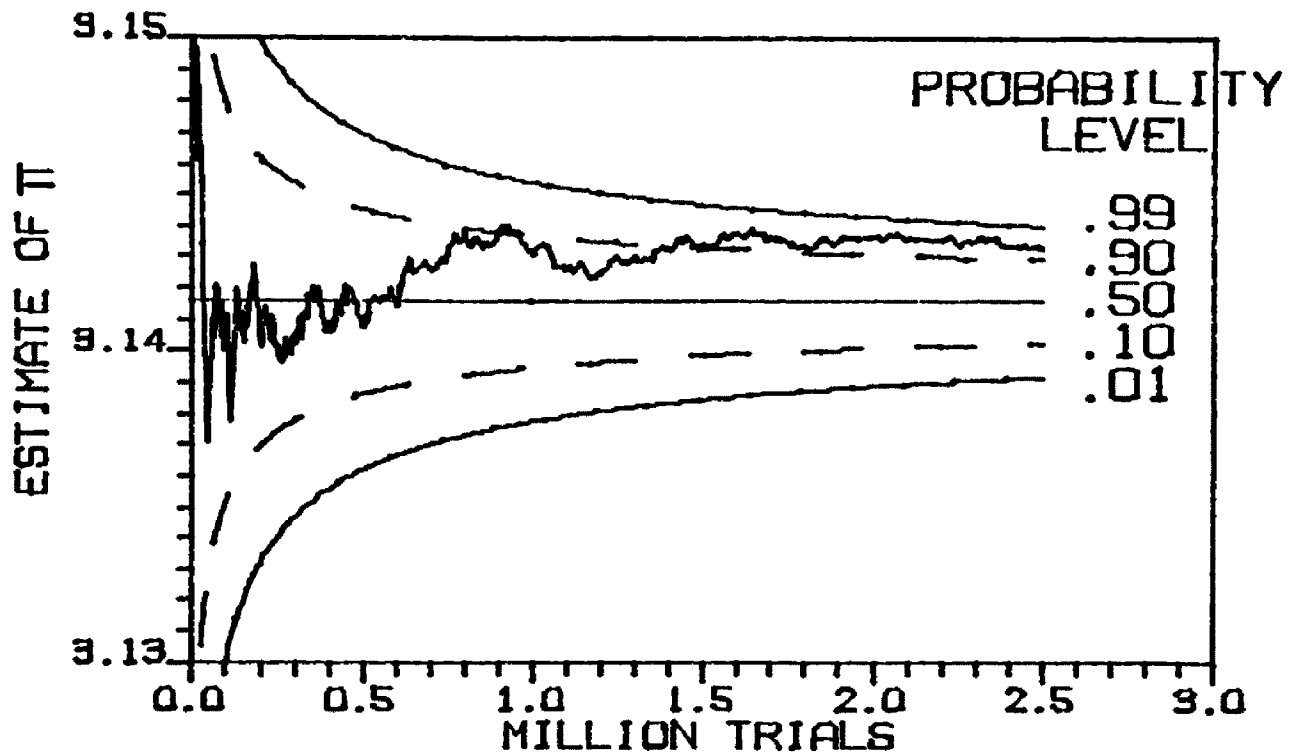


Figure 14a. Randu's approximation to π as a function of the number of points generated. The theoretical distribution of expected results is shown as well.

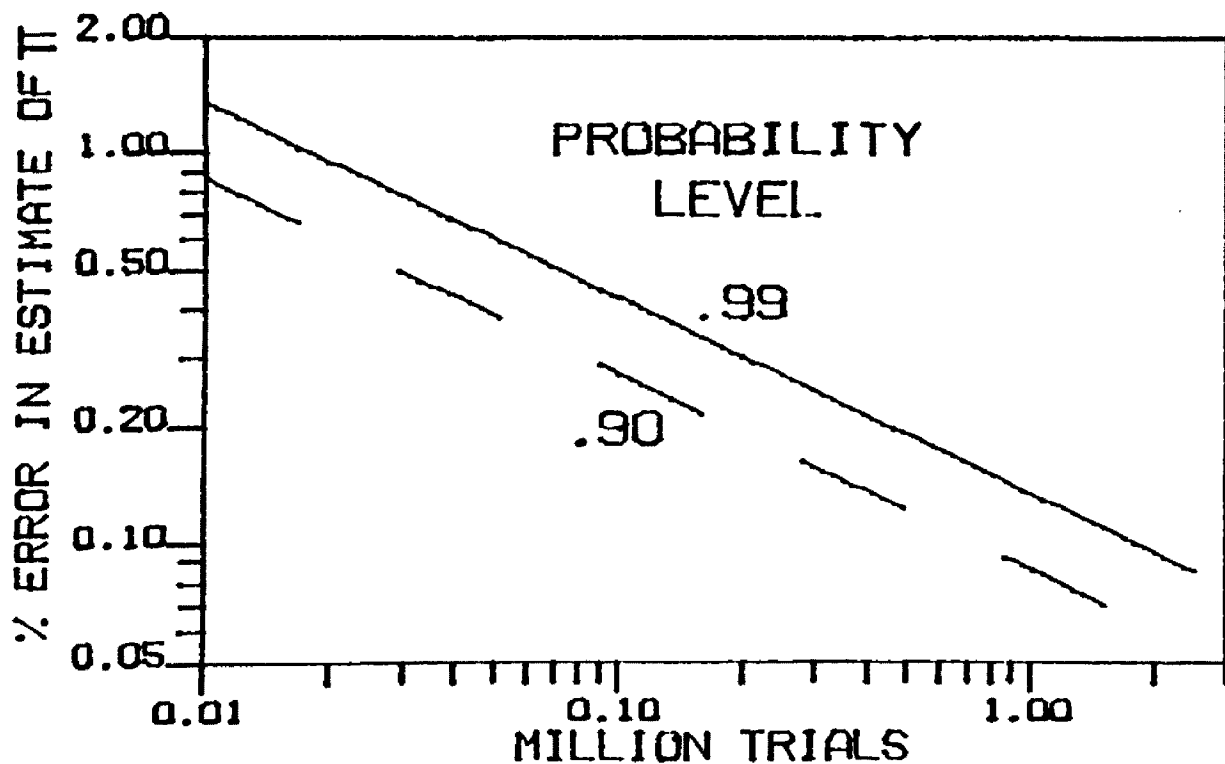


Figure 14b. The percentage error in the estimation of π represented by the .99 and .90 probability levels shown in Figure 14a.

Chapter 4

EXPERIMENTAL PROCEDURE

Data chosen for study

The raw data consisting of daily weather observations at all reporting eastern Montana weather stations were obtained from the National Oceanic and Atmospheric Administration. These data go back to 1900 for a few stations, but the data prior to 1910 are, in general, very broken, with few stations reporting regularly. The stations with the longest unbroken histories were selected for analysis. These were Billings, Busby, Crow Agency, and Miles City.

Since each site has an unbroken record dating from at least 1911, this date was picked as the beginning of the time series analysis. For those statistical analyses that do not require unbroken records of equal length, all the available data from each station were utilized. The records of Billings, Busby, Crow Agency and Miles City began in 1905, 1910, 1900 and 1900 respectively. The terminus of the time series was dictated by the availability of the latest data and December 1976 was chosen as the end of the daily precipitation series and December 1979 was the terminus of the monthly series.

Although this period of 70 - 80 years may be representative of the types of climates that can be expected in the next few decades, the nature of longer term climatic changes was not investigated in this paper.

Preliminary statistical analysis

As a preliminary characterization of the precipitation levels of the region, the frequencies of occurrence of various amounts of daily total precipitation were first determined. This was accomplished by categorizing each daily observation from each of the four weather stations into the following size classes: No Rain; Trace; 0.01" - 0.05"; 0.06" - 0.10"; 0.11" - 0.20"; 0.21" - 0.30"; 0.31" - 0.50"; 0.51" - 0.75"; 0.76" - 0.99"; 1.00" - 1.25"; 1.26" - 1.50"; 1.51" - 1.75"; 1.76" - 1.99"; 2.00" - 2.99"; and 3 inches or greater. The observations were further categorized by the month of observation. The contributions to the total seasonal and annual amounts of precipitation from each precipitation size class were then determined. The seasons were defined to be: Winter = December, January, and February; Spring = March, April, and May; Summer = June, July, and August; Autumn = September, October, and November.

The distributions of the number of days between rains of various sizes were determined next by counting the number of days between rains of a trace or more, 0.01" or more, 0.05" or more, and 0.10" or more. The distributions of the lengths of dry spells for the individual months and seasons were then summarized.

Recognizing the interrelatedness of these parameters and wishing to simplify the analysis as much as possible, a single factor was desired for further study. It was felt that variations in the P/E index (defined in note below) would be the most comprehensive measure of climatic variability, combining the interactions of temperature and moisture into a single measure.

Temperature records were, unfortunately, too incomplete for the task as data were only available for the period 1950 thru 1976. However, since the mean annual temperature of the region is (weakly) inversely correlated with total annual precipitation (as shown in Figure 15: $r = -.17$, $p = 0.13$) and the P/E index is primarily influenced by the precipitation levels (as shown in Figure 16), it was felt that the P/E index is not that much more efficient a climatic indicator than just the total monthly precipitation. Consequently, the historical record of total monthly precipitation was subsequently chosen for a more detailed analysis of climatic variability.

As a preliminary characterization of the monthly precipitation patterns of the region, the means and standard deviations of the average monthly total precipitation were calculated for each station for all years of record.

Creation of time series

It was desired to quantify the magnitude of any long term changes in the mean monthly precipitation levels of the region, consequently the historical records of the total monthly precipitation from each weather station were next considered to be time series.

Note:

The P/E index was introduced by Thornthwaite (1931) and is defined to be the following function of monthly total precipitation (P_i) and mean Fahrenheit temperature (T_i):

$$P/E = 115 \cdot \sum_{i=1}^{12} (P_i / (T_i - 10))^{1.111}$$

The P/E index is a description of the relative aridity of an area, varying from less than 16 in desert areas, to over 100 in rain forests.

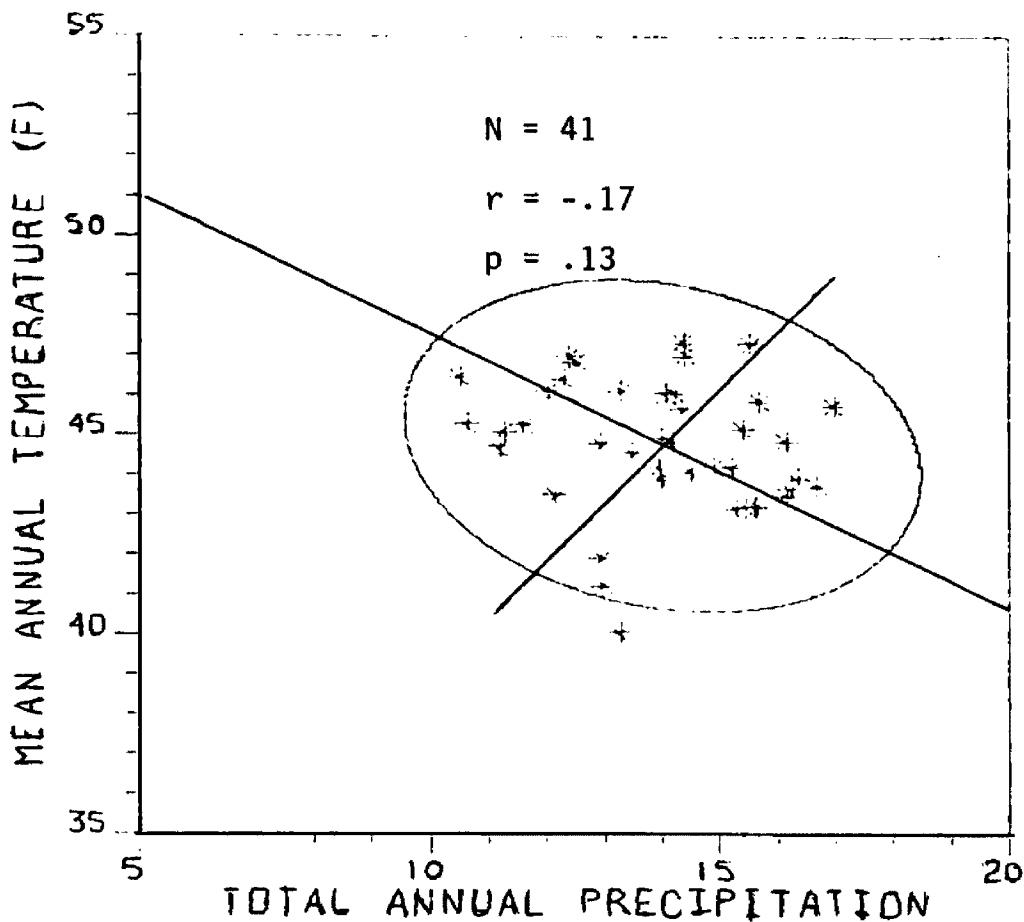


Figure 15. Correlation of average mean annual temperature and average mean annual precipitation for all weather stations and all years of record.

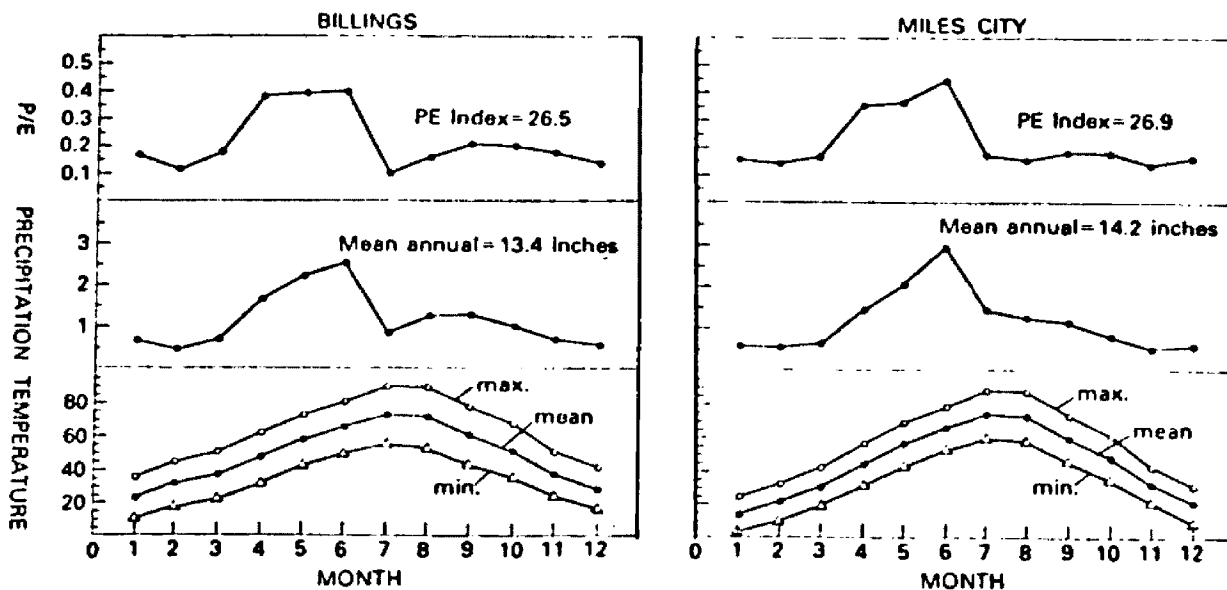


Figure 16. Relationships between temperature, precipitation and P/E indices for Billings and Miles City, 1950 - 1976. (First published in U.S.G.S., 1979)

Accordingly, the daily precipitation records of each site were first summed into 4 series of monthly totals, each series having 828 terms, which corresponds to 69 years of monthly values at a particular site. The monthly values for the period 1977 - 1979 were obtained from the monthly summaries prepared by National Oceanic and Atmospheric Administration.

Each time series was then normalized by taking the logarithm of each term, averaging these logarithms, and then subtracting the series' mean from each term and dividing by the series' standard deviation. Each station's series can be considered a time dependent series (i.e. the values are ordered according to time of observation) and these series are the starting point for the time series analysis to be carried out.

Fourier analysis of the time series

The discrete Fourier transform of each time series was first computed and the amplitudes for corresponding frequencies averaged together to produce a single, average Fourier transform, representative of the region's precipitation history.

Next, the statistical significances of these amplitudes were checked by the Monte-Carlo simulation technique. This was done as follows:

- 1) Each stations' time series was decomposed into twelve sub series, each one representing a single month at a single station. The mean and standard deviation of each subseries was computed. This results in twelve individual populations for each station, each

characterized by its own mean and standard deviation, each representing a single month at a given station.

2) 1,000 Monte-Carlo trials were run to evaluate the significance of the amplitudes of the observed average Fourier transform. Each trial consisted of the following:

a) A synthetic series for each station was constructed by generating random monthly deviates with a mean and standard deviation as required by the given month for a given station. Each of the four synthetic series consists of 828 random monthly terms, comprising 69 sets of 12 random monthly terms. This synthetic series has the same monthly averages and standard deviations as the actual series, but there is no relationship between succeeding terms, as this is the parameter to be investigated.

b) The Fourier transform of each synthetic series was computed and the corresponding amplitudes were averaged together. This produces a random, average Fourier transform.

3) The corresponding amplitudes in all the random average Fourier transforms were then pooled together, sorted and the .99, .95, .90, .50, .10, .05, and .01 critical values found for all amplitudes. These values were then compared with the actual average Fourier transform derived from the four observed monthly precipitation records to determine if any of the observed amplitudes were significant

Coherence analysis of time series

Construction of the average annual correlogram. To complement the above Fourier analysis, the nature of the correlograms of the four

stations' time series was investigated. This was accomplished by first obtaining the correlogram of each station's time series and then averaging the four correlograms. This resulted in an average correlogram, representative of the region. This correlogram was not very informative, however, because the intraannual variation in the monthly precipitation levels dominated the correlogram, making the presence of other periodic variations impossible to discern. It was desired, therefore, to sum each station's time series into yearly values, obtain the correlogram of the annual precipitation record for each station, and then average these correlograms as before, obtaining a correlogram showing the interannual variations only.

This requires the selection of a month to begin the precipitation year. In principle, any month could be used as the starting point for the year, however certain considerations limit the choice in practice. The variation in average monthly precipitation for two of the stations under consideration was shown in Figure 16. This figure reveals that there are two distinct phases of precipitation at these sites. The first is the Spring and Summer rains, lasting from February to July while the other is the Fall and Winter precipitation, lasting from July to January. These two periods represent different characteristic atmospheric circulation patterns existing over the Northern Great Plains at different times of the year (Rossby waves). February or July would, therefore, be logical choices as the start of the precipitation year. February was chosen because it allowed a slightly longer time series to be created.

The choice of a starting month is not a critical factor however, as the 12 possible correlograms based on each of the 12 month's serving as the start of the precipitation year are virtually identical in every detail.

Using February as the starting month then, each station's monthly time series was converted into an annual time series. The correlogram of each station was computed and the autocorrelation coefficients at corresponding lags in the 4 correlograms averaged together.

Significance of the average correlogram. The statistical significance of the average correlogram was tested in a manner exactly similar to the method used to test the statistical significance of the average Fourier transform.

- 1) The mean and standard deviation of each station's annual time series was determined.
- 2) 1,000 Monte Carlo trials were carried out. Each trial consisted of the following:
 - a) Four random series were constructed, each having the same mean and standard deviation as one of the 4 stations.
 - b) The correlogram of each synthetic series was computed and the corresponding autocorrelation coefficients in each of the 4 resulting correlograms averaged together.
- 3) The corresponding autocorrelation coefficients in each of the 1,000 resulting random, average correlograms were pooled together, and the distributions of the lags were computed.

Accuracy of Monte-Carlo estimates

To guard against any pathological random series from unduely influencing the distribution of observed statistics, the stability of the Monte Carlo simulations was tested.

First, different random number generators were employed to generate random series and these series had their Fourier transforms and correlograms taken in a manner exactly similar to the one described earlier. The distributions of the resulting Fourier amplitudes and autocorrelation coefficients were then compared to the ones obtained with the extensively tested random number generator.

Next, the randomization method of Fisher was employed to test the stability of the results of the above Monte-Carlo trials. In this procedure, the actual raw data is used as the source of random values by selecting at random monthly values and creating a synthetic series whose Fourier transforms and correlograms are computed. This was done for each station and the four resulting Fourier transforms were averaged together as were the four correlograms. This procedure is repeated a number of times, and the resulting average transforms tabulated as before.

Both of these checks indicated that the critical values given in this report are accurate to about 2 significant figures, an accuracy of about 1 percent.

Prediction of future precipitation patterns

Three different methods were used to determine the expected nature of future precipitation patterns. Basic statistical descriptions of each time series were first performed; determining the means, standard deviations, and distributions of both the growing season and annual precipitation levels. This allows the prediction of the limits of the expected precipitation levels, giving the maximum and minimum values expected, without saying anything about when these levels will be seen.

The second method of description was based on the observed number of days between rains of various sizes. Knowledge of the number of days per year with a given amount of rain or more and the distribution of the number of days between these rains allows one to determine how often any specified amount of time will pass between rains of a given magnitude. Once again, this type of analysis does not take the time of observation into account and consequently, the long term changes in this parameter cannot be determined.

The third method is based on the cycles found in the Fourier transformation. If the cycles in the Fourier transform are thought to be a result of some persistent feature of the climate, then they can be expected to persist into the near future. This provides an estimate of the time scale on which characteristic variations can be expected, while the magnitudes of these Fourier amplitudes provides an estimate of the magnitude of these cyclic changes.

Chapter 5

RESULTS

Statistical summaries

Table 1 presents the statistical summaries of the total seasonal and annual precipitation levels of the region.

Table 1

Statistical Summary of the Total Seasonal and Annual Precipitation
of All Weather Stations and All Years of Record

	Total Precipitation (Inches)				
	Winter	Spring	Summer	Fall	Annual
Sample Size	300	300	300	300	300
Maximum Value	5.70	10.96	12.80	8.95	26.21
Minimum Value	0.26	0.91	1.13	0.32	5.91
Average	1.78	4.40	4.85	3.12	14.15
Standard Deviation	0.89	2.00	2.12	1.66	3.73
Standard Error of Mean	0.05	0.12	0.12	0.10	0.22
Width of 95% Confidence Limit	0.10	0.23	0.24	0.19	0.42
5% Quantile	0.60	1.83	1.97	0.97	8.40
25% Quantile	1.10	2.97	3.25	1.98	11.37
50% Quantile (Median)	1.61	4.05	4.63	2.79	14.08
75% Quantile	2.22	5.14	6.06	3.89	16.46
95% Quantile	3.60	8.51	8.68	6.55	20.68
Skewness	1.16	1.04	0.90	1.06	0.37
Standard Error	0.14	0.14	0.14	0.14	0.14
Probability of Occurrence (%)	0.00	0.00	0.00	0.00	0.86
Kurtosis	1.89	1.00	1.18	1.13	0.21
Standard Error	0.28	0.28	0.28	0.28	0.28
Probability of Occurrence (%)	0.00	0.04	0.00	0.01	46.44

As can be seen from this table, the mean spring total precipitation is 4.4 inches and the 20 year minimum and maximum are 1.83 inches and 8.51 inches respectively. The mean annual total precipitation is 14.15 inches and the 20 year minimum and maximum are 8.4 inches and 20.68 inches respectively.

Figure 17 presents the histograms of the seasonal precipitation while Figure 18 presents the histogram of the total annual precipitation. As can be seen from these figures, winter is the driest season and also is the least variable in the expected amount of precipitation. This figure also reveals that summer is the wettest season and is also the most variable.

These seasonal totals are the result of individual precipitation events whose characterization is presented in Tables 2 and 3. Table 2 details the percent of all days on which precipitation of a given size or greater occurred. As can be seen from this table, a trace of precipitation (0.004") or more occur on approximately 30 percent of the days while approximately 10 percent of the days had greater than a tenth of an inch of precipitation. The spring and summer seasons have the most frequent rains which also accounts for their being the wettest seasons.

Since one day per year represents 0.27 percent of all the days in a year, it is also seen from this table that about once per year a rain of at least 1.25" occurs and once every five years a precipitation event occurs which deposits 2 inches of moisture or more in a single day.

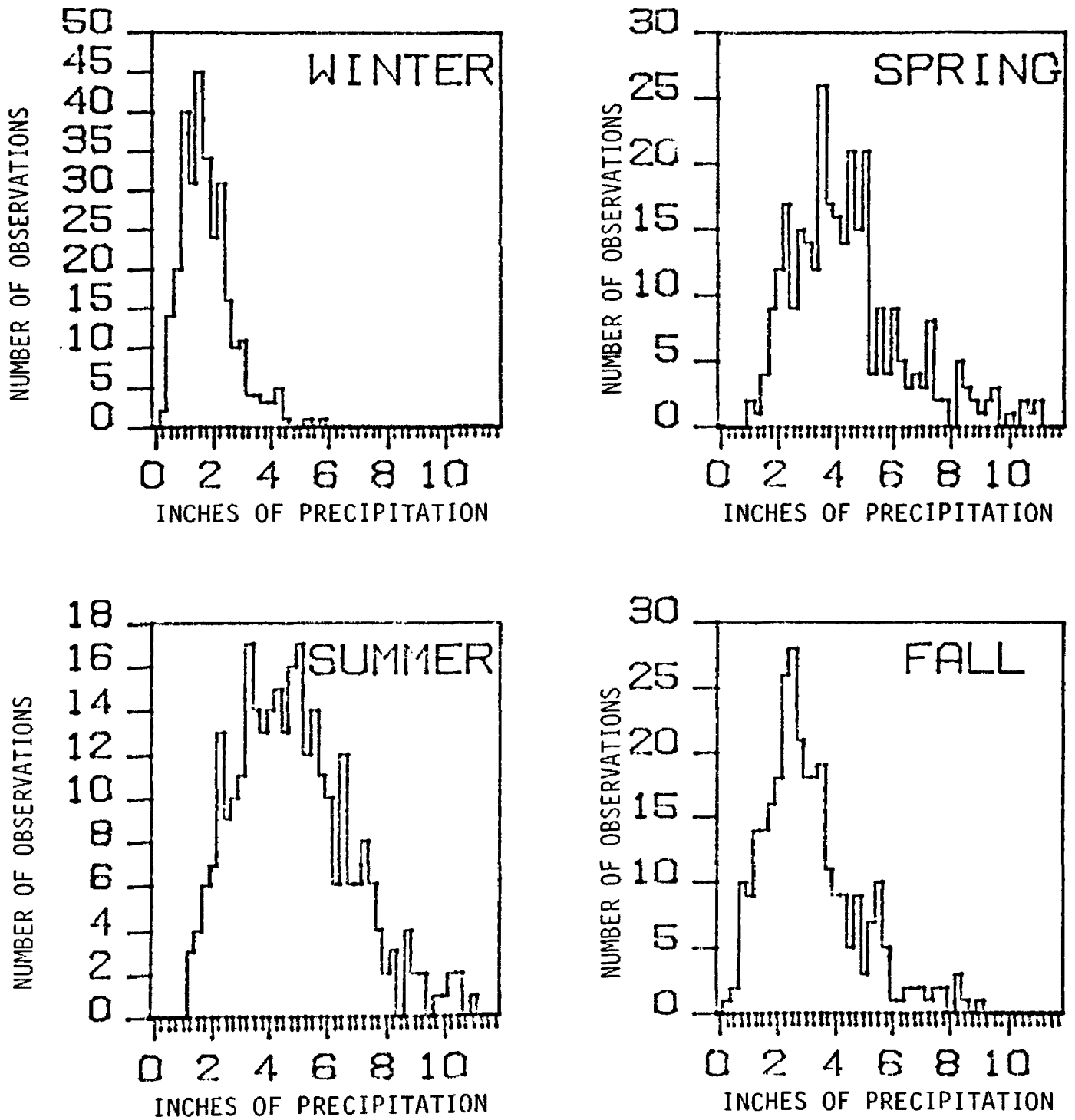


Figure 17. Histograms of total seasonal precipitation at all weather stations and all years of record.

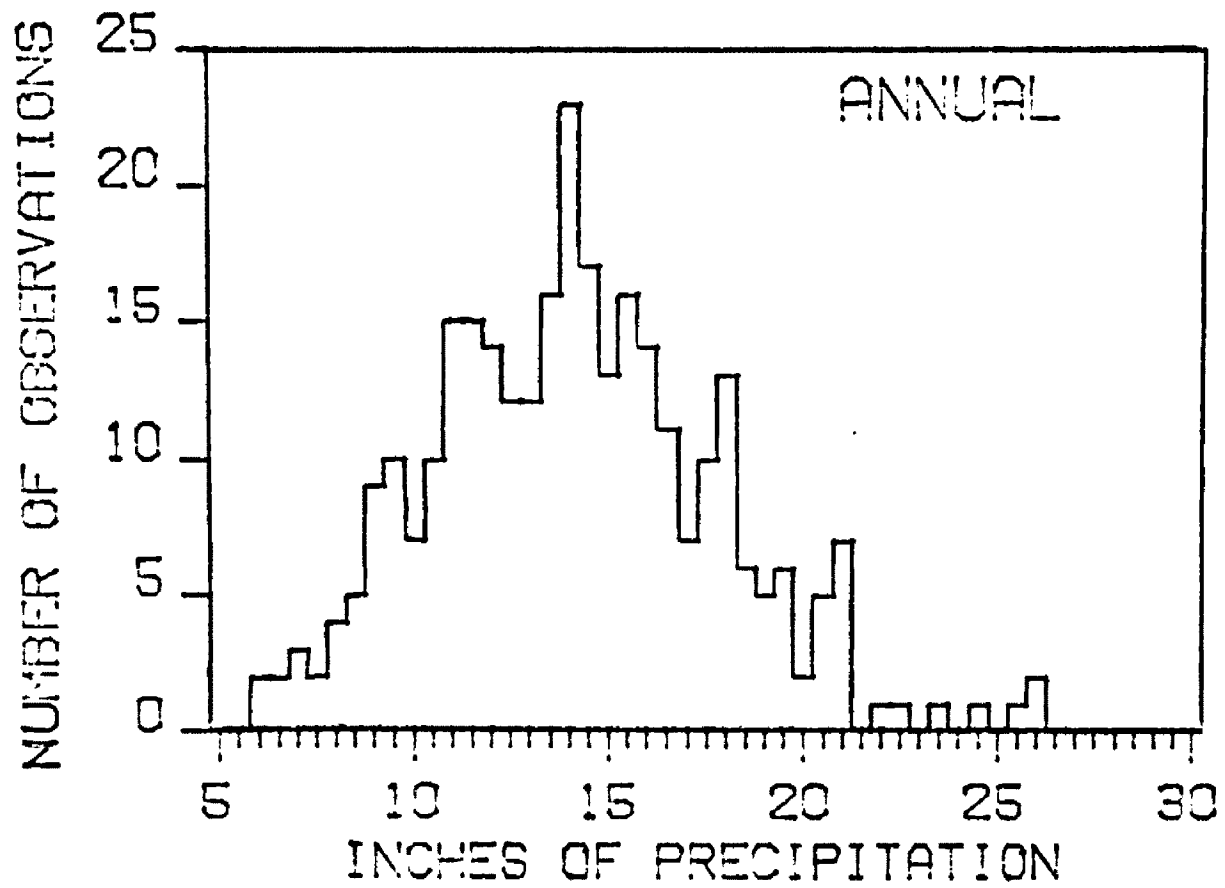


Figure 18. Histogram of total annual precipitation at all weather stations and all years of record.

Table 2

Percent of Days Having at Least Indicated Amounts of Precipitation

LOWER CLASS LIMIT	SEASON				
	WINTER	SPRING	SUMMER	AUTUMN	ANNUAL
0.004	31.384	35.484	30.450	25.430	30.686
0.010	19.856	25.149	22.545	17.536	21.277
0.060	10.036	16.209	15.314	11.013	13.160
0.110	5.713	11.522	11.634	7.960	9.228
0.210	2.415	6.899	7.648	4.756	5.449
0.310	1.013	4.348	5.473	3.077	3.494
0.510	0.259	2.105	2.977	1.521	1.726
0.760	0.082	0.965	1.498	0.757	0.830
1.000	0.027	0.503	0.790	0.359	0.423
1.260	0.016	0.248	0.427	0.224	0.230
1.510	0.000	0.145	0.265	0.100	0.128
1.760	0.000	0.095	0.159	0.062	0.080
2.000	0.000	0.076	0.087	0.050	0.054
3.000	0.000	0.011	0.015	0.004	0.008

Table 3

Percent of Total Precipitation From
Rains of at Least Indicated Size

LOWER CLASS LIMIT	SEASON				
	WINTER	SPRING	SUMMER	AUTUMN	ANNUAL
0.004	100.000	100.000	100.000	100.000	100.000
0.010	97.669	99.124	99.408	99.050	99.023
0.060	84.873	94.082	95.902	93.951	93.526
0.110	67.539	86.147	90.379	86.657	85.392
0.210	42.491	71.373	79.120	71.981	70.580
0.310	24.605	57.592	68.670	59.068	57.637
0.510	9.610	38.913	49.988	40.518	39.442
0.760	4.077	23.927	32.877	26.291	25.053
1.000	1.771	15.487	21.494	16.045	15.974
1.260	1.076	9.566	13.944	11.532	10.446
1.510	0.000	6.625	9.777	6.279	6.818
1.760	0.000	4.928	6.545	4.315	4.739
2.000	0.000	4.172	4.000	3.642	3.469
3.000	0.000	0.948	0.871	0.511	0.707

The relative contributions to the total precipitation made by the various precipitation size categories are presented in Table 3. This table details the percent of the total seasonal and annual precipitation that is due to events of various sizes or larger. It can be seen from this table that in the winter, most of the precipitation tends to be small events as 10 percent of all moisture comes from events greater than 1/2 inch while 40 percent of the spring moisture and 50 percent of the summer moisture comes from events greater than 0.5 inches. Over the course of a year, about 15 percent of the total moisture comes from events less than 0.1 inches and 15 percent comes from events greater than 1 inch.

The annual data presented in these two tables are graphically portrayed in Figure 19 and demonstrates the relationship between these two tables.

Summary of the number of days between rains

The frequencies of occurrence of dry spells of various durations are presented in Table 4. Dry spells are defined to be periods of time with no precipitation greater than or equal to 0.01 inches, 0.05 inches, and 0.10 inches occurring on a single day. Table 4 presents the number of times a year that a dry spell of various durations can be expected to occur for each of the 3 above mentioned daily precipitation limits. The first column of this table lists the minimum duration of a dry spell while the next 3 columns list the number of times per year that at least the one of days given in column number one will pass with no precipitation exceeding the limits given at the top of these 3 columns.

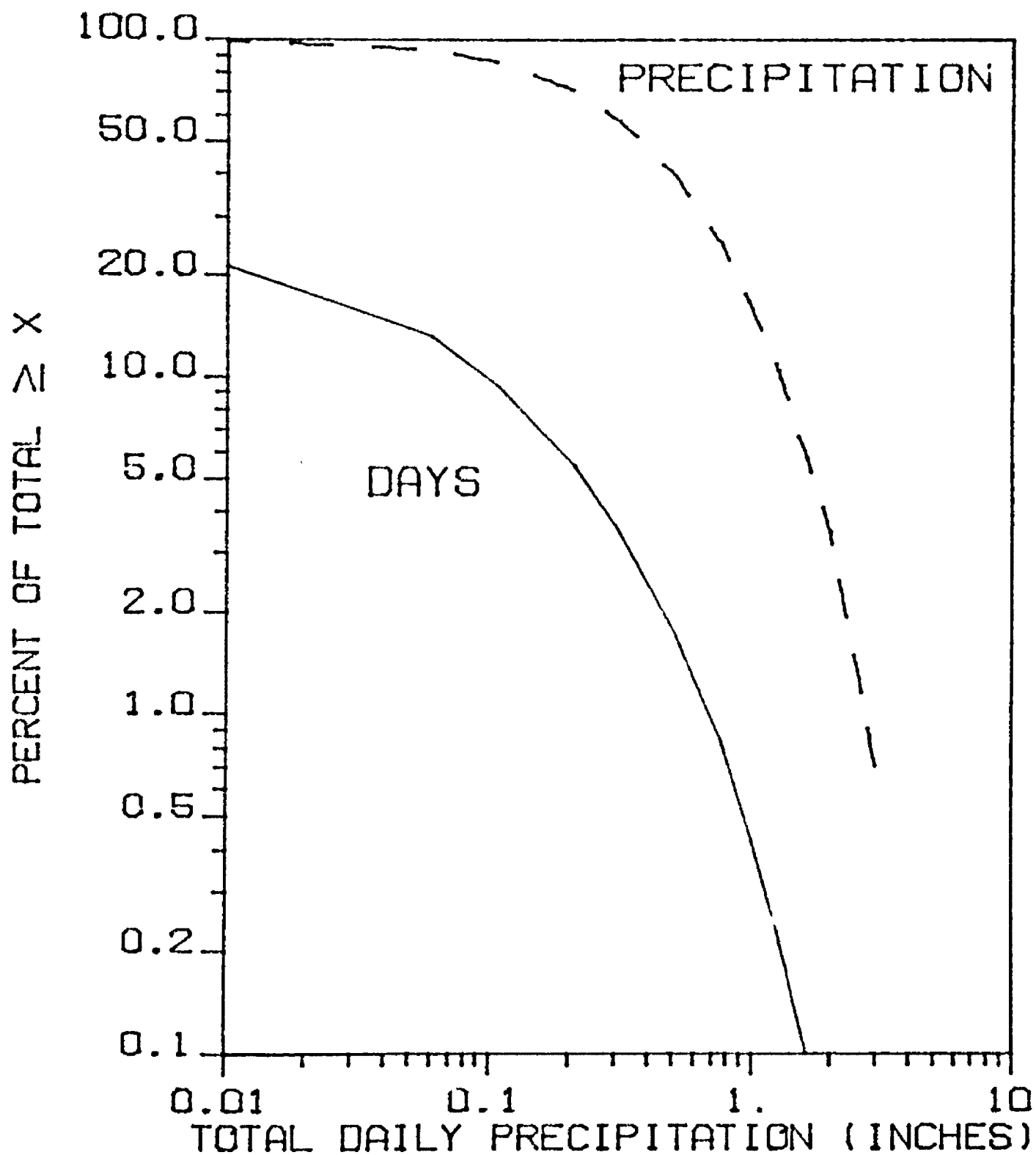


Figure 19. Percent of days with at least a given amount of precipitation and the percent of the total annual precipitation due to these events.

Table 4

Number of Times per Year That a Specified Number of Days or More Will Pass
Between Precipitation Events of at Least 0.01, 0.05 and 0.10 Inches.

NUMBER OF DAYS BETWEEN RAINS (LOWER-UPPER LIMIT)	SIZE OF PRECIPITATION EVENT (INCHES)		
	0.01 OR MORE	0.05 OR MORE	0.10 OR MORE
0	77.7140	48.0670	33.7050
1	46.7846	33.8877	25.5619
2	37.2320	28.7715	22.5224
3	29.9619	24.6920	20.0009
4	24.5250	21.2571	17.8829
5	20.1178	18.5543	16.1359
6	16.7730	16.2058	14.5710
7	14.1673	14.3581	13.2144
8	11.9439	12.6277	11.8547
9	10.2279	11.2160	10.7637
10	8.7397	9.9210	9.7748
11	7.4209	8.8280	8.9814
12	6.2816	7.7513	8.2230
13	5.4656	6.9024	7.5769
14	4.7693	6.1285	6.9817
15-16	4.0901	5.4292	6.4282
17-18	3.1194	4.3847	5.4393
19-20	2.3143	3.5132	4.6553
21-30	1.7758	2.8754	4.0092
31-40	0.5277	1.1483	1.8973
41-50	0.1826	0.4456	1.0047
51-60	0.0560	0.2081	0.5278
61-70	0.0280	0.1072	0.3006
71-89	0.0140	0.0423	0.1631
90 OR MORE	0.0039	0.0034	0.0640

For example, it can be seen from this table that 47 times a year one or more days will pass with no precipitation occurring on any one day greater than or equal to 0.01 inches. Similarly, 26 times per year one or more days will pass with no precipitation occurring greater than or equal to 0.10 inches. It can also be seen from this table that 7 times per year at least two weeks will pass with no precipitation occurring greater than or equal to 0.10 inches. It is also seen in this table that once per year at least 41 days will pass with no precipitation occurring greater than or equal to 0.10 inches. Similarly 0.06 times per year (or once every 15 years) 90 days or more will pass with no precipitation occurring greater than 0.10 inches.

This table is graphically portrayed in Figure 20. It can be seen from this figure that long dry spells do occur with some regularity and is one reason that the area is semiarid.

Time series analysis

The historical record of total seasonal precipitation for each the stations under consideration, i.e. Billings, Busby, Crow Agency and Miles City, are graphed in Figure 21 while the average Fourier transform of these stations monthly precipitation record is shown in Figure 22. A brief examination of these stations' total precipitation records reveal a few interesting features they all have in common. The first and most pronounced is the regular, large variation in the seasonal totals, with the spring season normally being the wettest season. This regular seasonal variation in the precipitation levels produces a large peak in the average Fourier transformation at the one year period. This is the

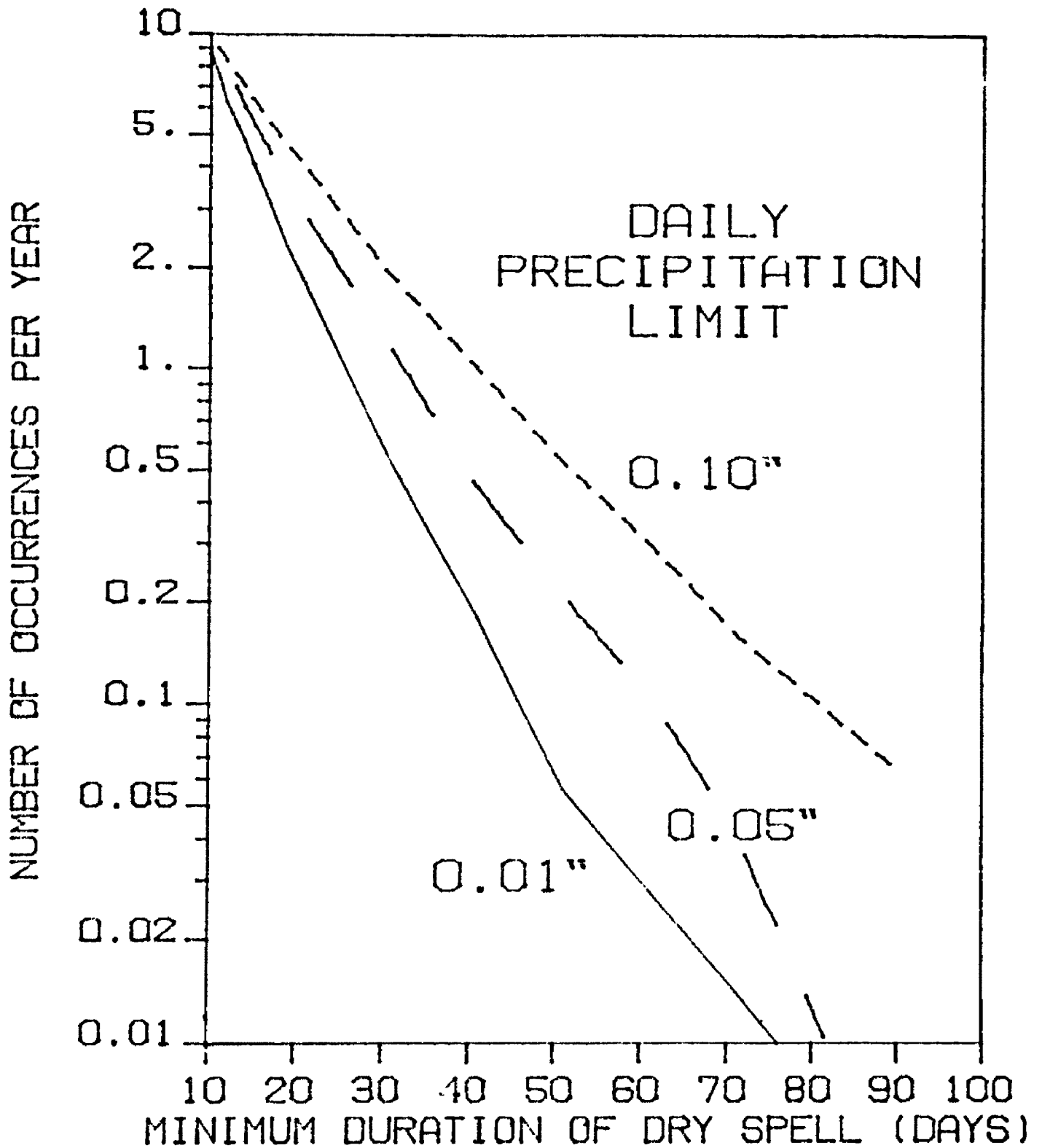


Figure 19. Number of occurrences per year of dry spells of various durations.

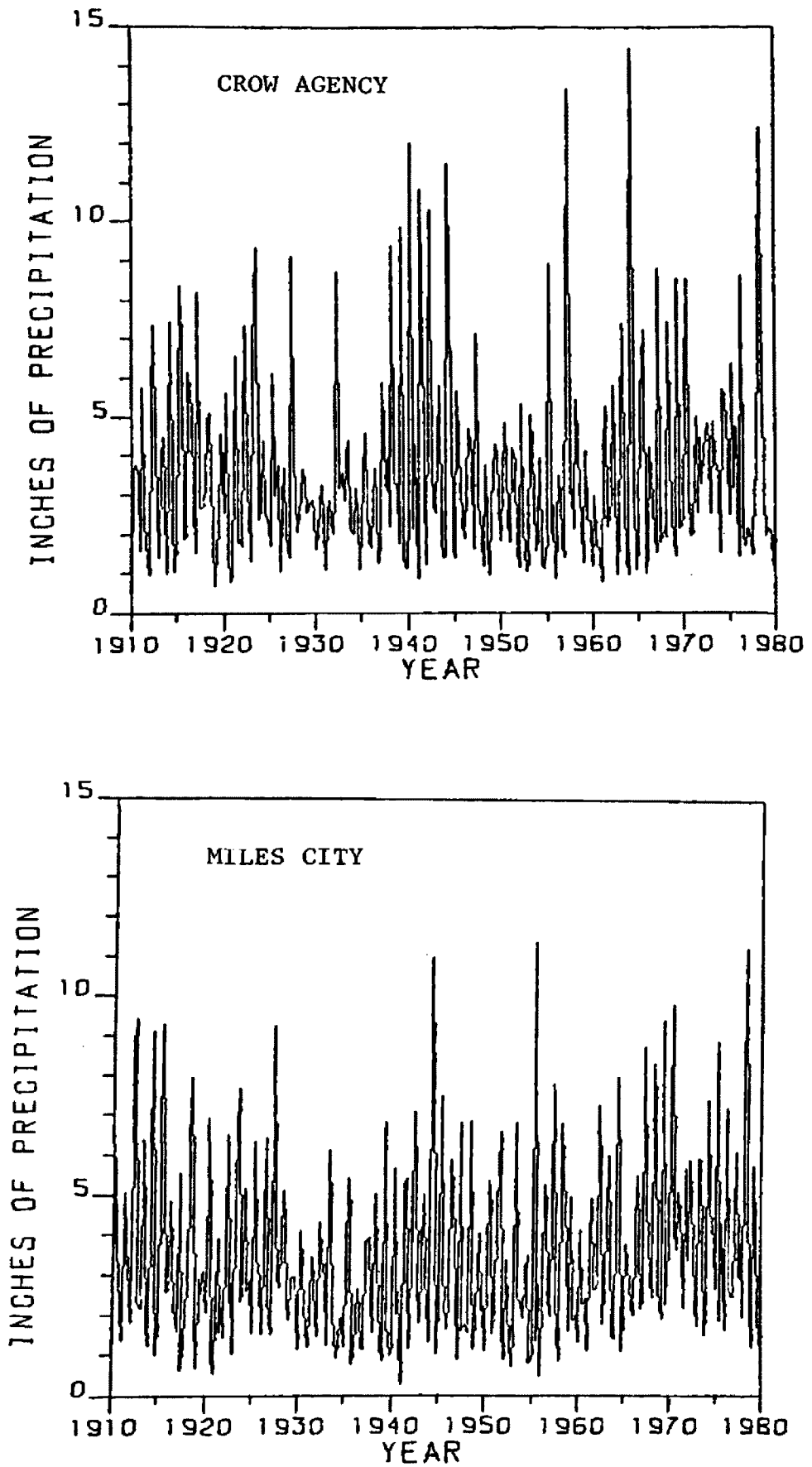


Figure 21. Historical records of seasonal precipitation.

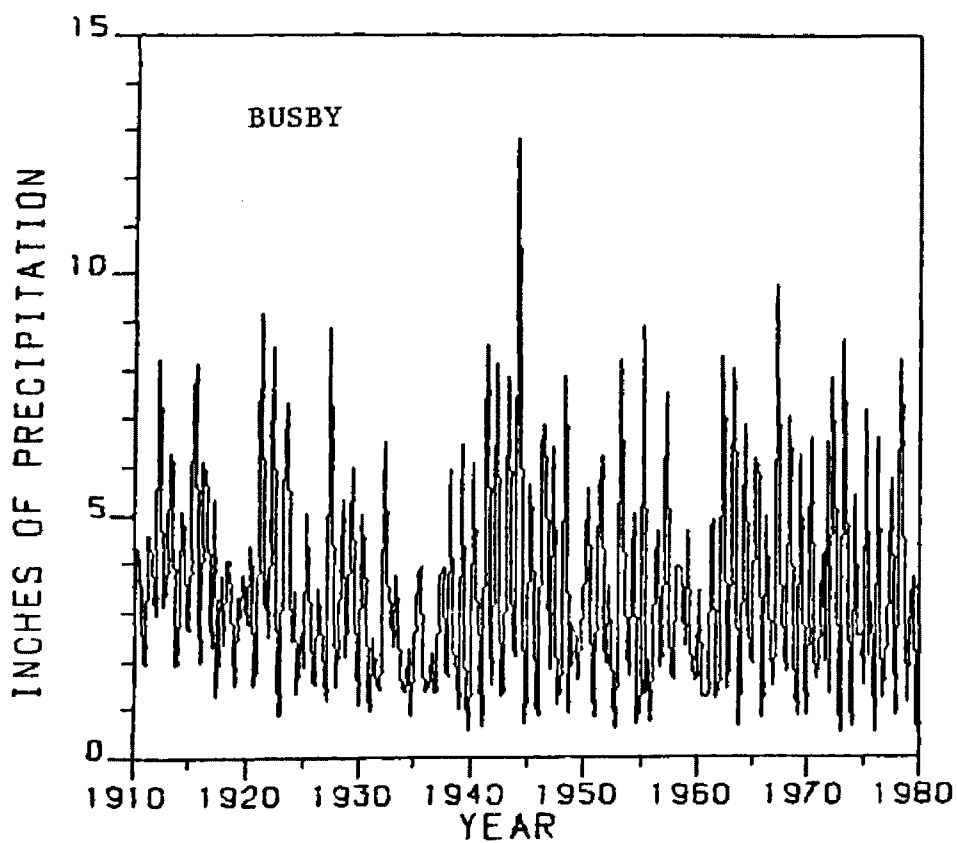
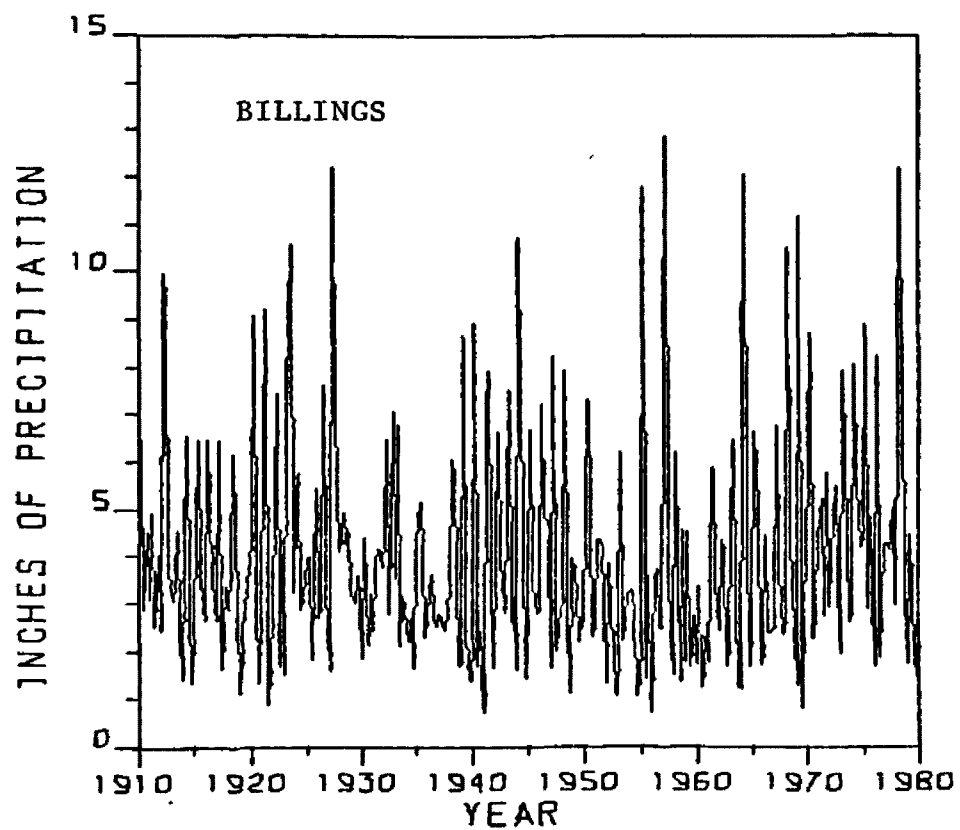


Figure 21. Historical records of seasonal precipitation.
(cont.)

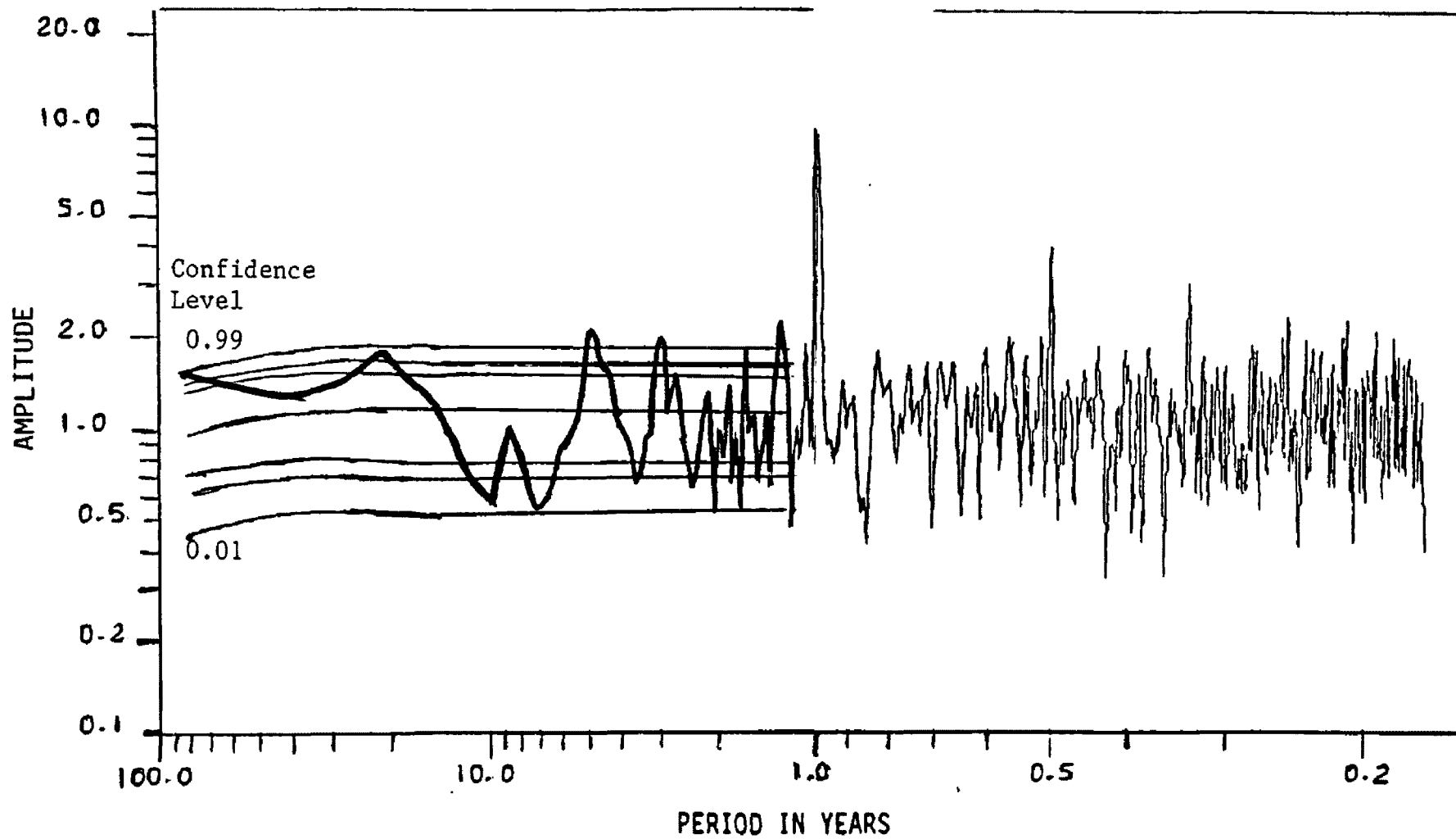


Figure 22. Average Fourier transform of region's seasonal precipitation record with 0.99, 0.95, 0.90, 0.50, 0.10, 0.05, and 0.01 critical values.

annual variation in the monthly precipitation that will serve as a measure of all other variations. The next feature that they all have in common is the dry period lasting from 1935 to 1937, the dry period in 1957-1959, and the wet period beginning from 1970. The timing of these periods suggests a 22 year period may be present, and a peak is seen in the average Fourier transformation at the 21.33 year period.

Although the 21 period is seen in the average Fourier transformation, the largest two peaks in the spectrum are the ones located at 5 and 3 years. If they are considered as two singlets then they correspond to two climatic forces, one of 5 years in period and the other of 3 years. If these two peaks are considered a doublet then they correspond to two interacting climatic forces, one having a periodicity of 3.75 years and another of 1.9 years.

This is a demonstration that there is no way to unscramble the causes of these variation from just the Fourier transformation. It is these three periodicities (21, 5 and, 3 years) that predominate the average transform (Figure 22) for periods greater than 1 year.

The statistical significances of the average Fourier transform is shown in Figure 22 as well. The critical levels shown in this figure represent the expected distributions of the amplitudes of the average Fourier transform if there were no periodicities with length other than 1 year present, and if there was no persistence present either. The 0.01, 0.05, 0.10, 0.50, 0.90, 0.95, 0.99 critical values of the null average Fourier transform are shown in this figure. It is the distribution of the amplitudes of this null transformation that was determined via the Monte-Carlo simulation.

It is also seen from this figure that the amplitude corresponding to 85 years is also seen to be significant at the 0.05 probability level. This period is, however, the longest period that can be resolved via the Fourier transformation and it is uncertain whether there is truly a periodicity of length 85 years in the data or not. This peak could be the result of any periodicities of any length greater than 85 years; even linear trends present in the data would appear at this period. Simple persistence could also be responsible.

A word on the stated probability levels corresponding to various critical values is in order here. The critical values are correct only if you have some a priori reason to look at a given period to see if there is a peak there. If you just scan all the amplitudes and stop at the largest, the the stated probability level will be too high and the distribution of the maximum amplitude of all periods greater than one year should be consulted for the probability of a given amplitude anywhere in the spectrum.

Since all Fourier transformations have a maximum amplitude somewhere, we should compare of observed maximum amplitude with the null distribution of the maximum amplitude to see if the observed maximum is significantly larger than the expected maximum. The critical values of the maximum amplitude for all periods longer than 1 year is shown in Figure 23, superimposed upon the observed amplitudes of the average Fourier transformation of the region's monthly precipitation record. We see from this figure that none of the amplitudes are significant at the 0.10 level, indicating that they are no larger than the expected maximum amplitude if there were no reason to look at any particular period ahead

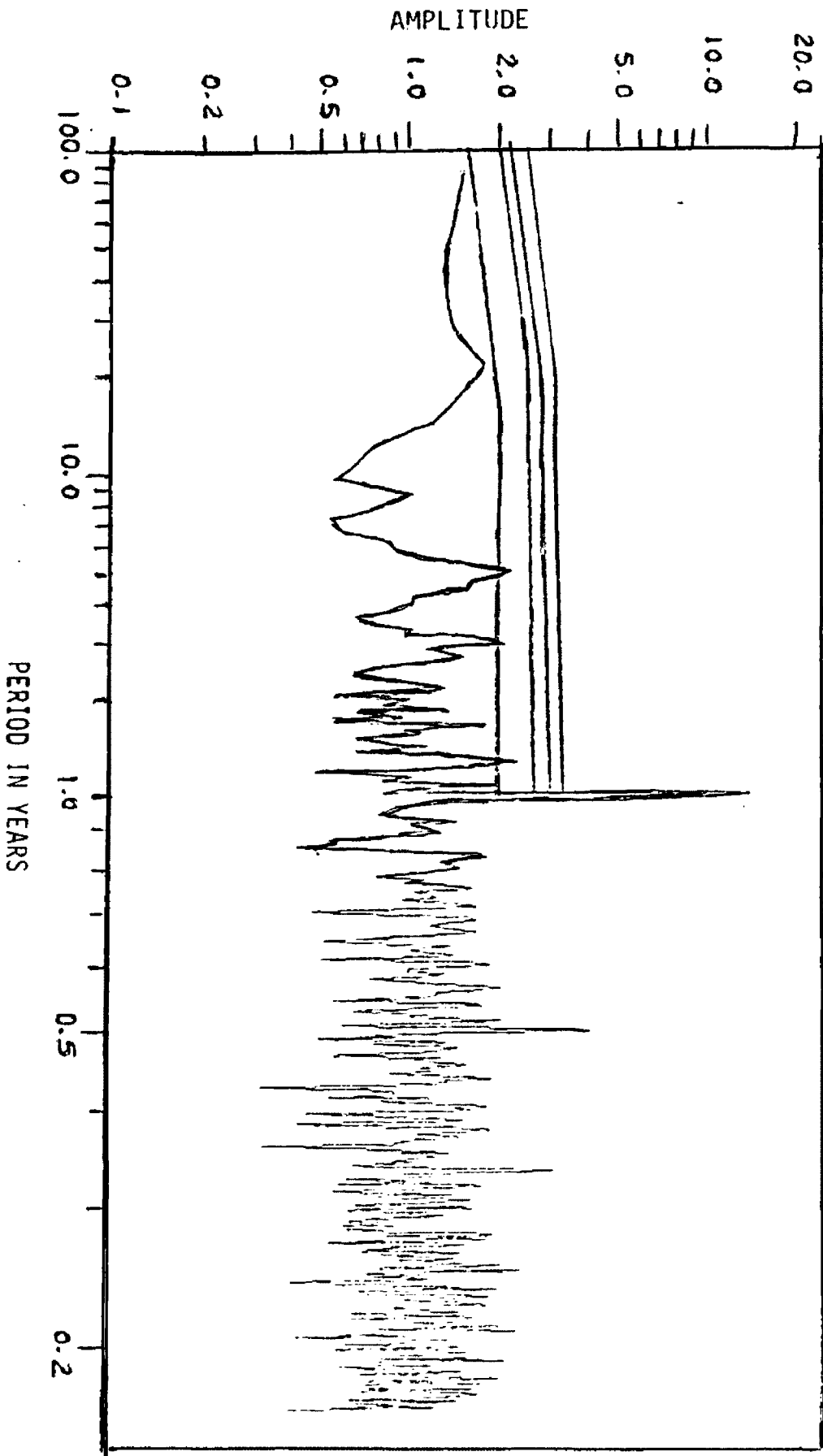


Figure 23. Average Fourier transform of region with 0.99, 0.95, 0.90, and 0.50 confidence limits of maximum amplitude of period greater than one year.

of time.

Coherence analysis

Figure 26 shows the average correlogram of the region. To gain some idea of how large these average autocorrelation coefficients are compared with the expected average correlograms of 4 random series, the null distribution of the average autocorrelation coefficients were worked out via the Monte-Carlo simulation technique described earlier. The results of this process are also shown in Figure 26. The autocorrelations are seen to rise and fall with a period of about 5 years, corresponding to the largest peak in the Fourier transform. The 21 year sine wave is seen very weakly as a gentle rise and fall of the overall correlogram.

For truly periodic series it was seen that the autocorrelation coefficients do not vanish with increasing lag but are themselves periodic. For Markoff series, the autocorrelation coefficients decrease with increasing lag. The case here is more closely related to the cyclic variation, and the major period of fluctuation is the 5 year period that was dominant in the Fourier transform.

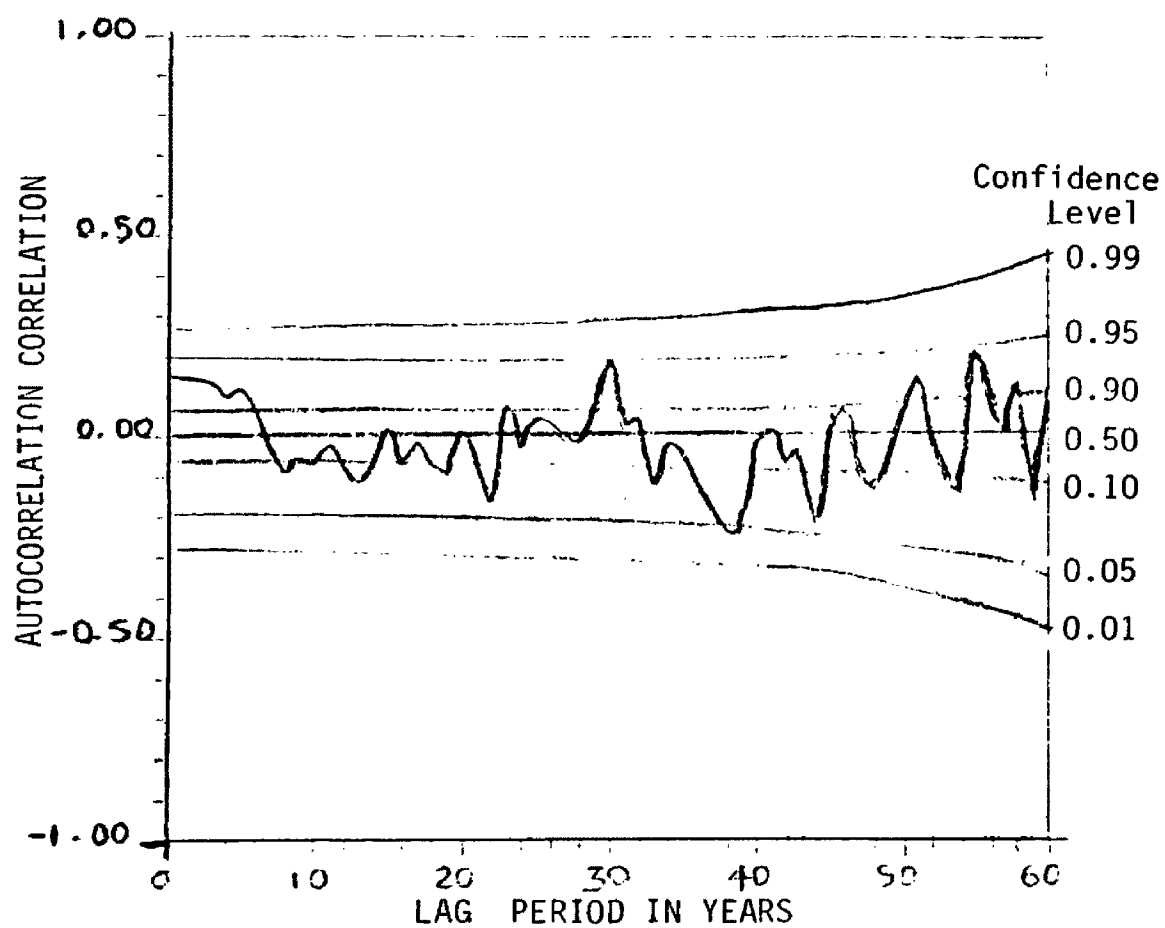


Figure 24. Average correlogram of region with 0.99, 0.95, 0.90, .50, 0.10, 0.05 and 0.01 confidence limits.

Chapter 6

DISCUSSION

Limitations of the data base

This study characterized the climate of the region via its historical record of precipitation. These data began in 1900 for two of the four stations under study while the other two stations began recording precipitation data in 1910. Climatic changes occurring over time periods ranging from centuries to millenia are therefore unquantifiable. Climatic indicators that have historical records extending back thousands of years must be studied to put any long term climatic changes into perspective. Historical records of tree ring widths are one obvious example of available climatic indicators useful towards this end.

Mathematical procedures

The Fourier transform and the correlogram are seen to be two useful methods by which the characteristic time scales of climatic change can be determined. Due to the essentially unquantifiable nature of the Earth's climatic system however, it is impossible to unambiguously determine, based exclusively on these two procedures, the causal mechanisms of any observed peaks in either the Fourier transform or the correlogram.

The Monte-Carlo simulation technique utilized in this study provides a convenient method of determining the distribution of any statistic of interest. This is true regardless of the degree of complexity of the procedure by which the statistic is arrived at.

Often in a large scale climatological study the historical records of various types of data from many different locations must be combined. These data sometimes have differing distributions, missing values or any number of other features which require transformations or other preliminary treatments of the data prior to analysis. These preliminary manipulations can easily render an analytical determination of the distribution of a particular statistic impossible.

With the Monte-Carlo simulation procedure any statistic can have its distribution determined by merely using random numbers in place of the data under study. By then performing the same operations on the random data that were performed on the actual data, the distribution of any statistic can be determined.

Climatological analysis

The climate of this region is seen to be very variable and on the average can be considered semiarid. The median annual total precipitation is 14.1 inches with the 5% and 95% quantiles being 8.4 inches and 20.7 inches respectively. The median total spring precipitation is 4 inches with an expected range of 2 to 9 inches within a 20 year period.

Rains between 0.10 inch and 1 inch account for 70 percent of this total with 15 percent of the total falling in rains less than 0.10 inch and 15 percent falling in rains greater than 1 inch. Precipitation falling in daily amounts less than 0.10 inches and greater than 1 inch will have less effectiveness (on a per inch basis) than precipitation falling in amounts between these limits due to the evaporation of small rains and the runoff of large rains. Daily precipitation events of 1 inch or greater occur about 3 times every two years, events of 2 inches or greater occur on the average once every 5 years and events of 3 inches or greater occur about once every 30 years.

Rain fall occurs on 1 day in 3 with 4.5 days being the median number of days between rains of 0.10 inches or more. The amount of precipitation occurring during any particular time period is very variable however as droughts are a common feature of this region.

Twice a year a period of a month or more passes without any precipitation occurring greater than 0.10 inches. Once every 15 years over 90 days can be expected to pass without any precipitation of this size or greater falling.

The climate demonstrates long term cyclic variations in the amount of total monthly precipitation with recurrence intervals of 3, 5, and 21 years. The amount of variation represented by each of these long term cycles is about 20 percent of the annual variation in the monthly precipitation levels.

This variable, semiarid climate can interact with the poor soils of the region to render successful reclamation problematic. About 65 percent of the soils in the study area are Entisols which have very little profile development. About 15 percent of the soils are Mollisols, which have well developed A or surface horizons and about 20 percent of the soils are Aridisols, which have moderately developed A and B horizons. If disturbed, none of these soils will regain their original structure and profile under the present climate, as they were formed mainly during the late Pleistocene, under wetter and cooler conditions (U.S.D.A., 1975).

Typical strip mines leave a number of relatively large (up to 10 acres) depressions of up to 100 feet in depth in the restored surface. These depressions can accumulate sediment and runoff during seasons with high precipitation, forming a mud hazard to cattle, and possibly to deer and antelope (U.S.G.S., 1979). These soils also have high sodium contents which causes crusting of the soil's surface and restricted permeability to water (Sandoval and Gould, 1978). This results in water running over the surface of the soils rather than percolating through them, thereby reducing the water available to growing vegetation. Due to the low annual total precipitation, salt accumulation in the top soils will be a continual problem in the area.

Natural revegetation of disturbed areas in this region is very slow, requiring many decades to reestablish a climax plant community (Olson, 1973). Fifty-year-old spoils in the region show some near-climax communities and some communities in the initial stages of succession. If soil and environmental conditions at each proposed

mining site were carefully studied before and during mining however, and the proper reclamation techniques applied, the chances of successful reclamation seem fair to good although decades to centuries will be required to either prove or disprove this point (U.S.G.S., 1979).

The three major peaks in the Fourier transformation (3, 5 and, 20 years) demonstrate the presence of long term variations in the climate. If we consider these sine waves to be the result of some persistent feature of the climate, then we might assume that these periodicities will continue into the near future. These periodicities can interact to produce characteristic time periods of variation on the order of centuries, and indeed the 85 year variation in the monthly precipitation record seen in the Fourier transformation of the region's precipitation history (Figure 22) may be a consequence of these shorter variations passing in and out of phase.

Although the cause of this periodic climatic variation is open to question, its consequences are not as speculative. Species live in areas where they can successfully reproduce over a number of generations. If an organism cannot cope with the range of environmental variability indigenous to an area, it must adapt its life style in some way. During adverse times, species with the ability to migrate to more hospitable areas do so. Some enter a period of dormancy to wait out the bad times, while others create a habitable microclimate to ensure their survival. In areas with periodic drought, all organisms unable to cope with drought will perish. The historical record of Eastern Montana shows a climatic variability that must be recognized and adapted to in any agricultural pursuit. The droughts of the 1930's and late 1950's

are not unusual times hoped to never come again. They are, rather normal, persistent features of the environment which shall come again.

The grassland communities existing in this region have had hundreds of years to adjust to these conditions. The communities that will become reestablished on reclaimed soils will not have had this opportunity and consequently their long term stability is in question.

LITERATURE CITED

- Abbot, C. G. 1976. Smithsonian Miscellaneous Collection 448(7).
- Alvarez, L. W., W. Alvarez, F. Asaro, and H. V. Michel. 1980. Extraterrestrial cause for the Cretaceous-Tertiary Extinction. *Science* 208(4448):1095-1108.
- ✓ Berger, A. L. 1978. Long term variations of caloric insolation resulting from the Earth's orbital elements. *Quaternary Research* 9:139-67.
- Box, G. E., and M. E. Muller. 1958. A note on the generation of random normal deviates. *Ann. Math. Statist.* 29:610-11.
- Bradley, R. S. 1976. *Precipitation History of the Rocky Mountain States.* Westview Press, Boulder, Colorado.
- Bray, J. R. 1974. Vulcanism and glaciation during the last 40 millennia. *Nature(London)* 252:679-80.
- Brigham, E. O. 1974. *The Fast Fourier transform.* Prentice - Hall, Inc. Englewood Cliffs, New Jersey.
- Bryson, R. 1974. A perspective on climatic change. *Science* 184:753-60.
- Budyko, M. I. 1977a. *Climatic Changes.* American Geophysical Union. Washington D.C.
- _____, 1977b. On present day climatic changes. *Teilus* 29:193-204.
- ✓ Charney, J. G. 1974. Dynamics of Deserts and Drought in the Sahel. *Quarterly Journal of the Royal Meteorological Society*, 101:193-202.
- Conover, W. J. 1971. *Practical nonparametric statistics.* John Wiley and Sons Inc. New York, New York.
- Cooley, J. W., and J. W. Tukey. 1965. An algorithm for the machine calculation of complex Fourier series. *Mathematics of Computation* 19:297-301.

- Diaz, H. F., and R. G. Quayle. 1980. The climate of the United States since 1895: spatial and temporal changes. *Monthly weather review* 108:249-66.
- Dicke R. H. 1979. Solar luminosity and the sunspot cycle. *Nature* 280:24-27.
- Douglass, A. E. 1919. *Climatic Cycles and Tree Growth*. Vols 1-3. Carnegie Institution of Washington, D. C.
- Eddy, J. A. 1976. The Maunder Minimum. *Science* 192(4245):1189-1202.
- Flohn, H. 1979. On time scales and causes of abrupt paleoclimatic events. *Quaternary Research* 12(1):135-50.
- Frankignoul, C., and K. Hasselmann. 1976. Stochastic climatic models, Part II. Applications to sea surface temperature anomalies. *Teilus* 28:480-5
- Gribbin, J., ed. 1978. *Climatic Change*. Cambridge University Press. Cambridge, England.
- Hansen, J. E., W. Wang, and A. A. Lacis. 1978. Mount Agung eruption provides test of a global climatic perturbation. *Science* 199:1065-1068.
- Hasselmann, K. 1976. Stochastic climatic models, Part I. Theory. *Teilus* 28:473-80.
- Hayes, J. D., J. Imbrie, and N. J. Shackleton. 1976. Variation in the Earth's orbit: Pacemaker of the Ice ages. *Science* 194(4270):1121-31.
- Hecht, A. D. et al. 1979. Paleoclimatic research: Status and opportunities. *Quaternary Research* 12:6-17.
- Hibler, W. D. III, and S. J. Johnsen. 1979. The 20 year cycle in Greenland ice core records. *Nature* 280:481-483.
- Hirschboeck, K. K. 1980. A new world wide chronology of volcanic eruptions. *Paleogeography, Paleoclimatology, Paleoecology* 29(1979/1980):223-241.
- Hsu, K. J. 1980. Terrestrial catastrophe caused by cometary impact at the end of Cretaceous. *Nature* 285:201-3.
- Johnson, S. J., W. Dansgaard, and R. G. Barry. 1975. Oxygen isotopes profiles through the Antarctic and Greenland ice sheets. *Nature* 235:429-34.

- Kneuth, D. E. 1969. The art of computer programming. Addison - Wesley Publishing Co. Reading, Massachusetts.
- Kominz, M. A., and N. G. Pisias. 1979. Pleistocene climate: deterministic or stochastic? Science 204:171-3.
- Kukla, G. J. 1975. Missing link between Milankovitch and climate. Nature 253:600-603.
- Lamb, H. H. 1970. Volcanic dust in the atmosphere with chronology and assessment of its meteorological significance. Philosophical Transactions of the Royal Society 266:425-533.
- Loder, J. W., and C. J. Garrett. 1978. Journal of Geophysical Research 83:1967-70.
- Lorenz, E. N. 1970. Climatic change as a mathematical problem. Journal of applied meteorology 9:325-329.
- _____, 1968. Climatic determinism. Meteorological Monographs 8, No. 3. American Meteorological Society.
- Manabe, S., and R. T. Wetherald. 1975. The effects of doubling the carbon dioxide concentrations on the climate of a general circulation model. Journal of Atmospheric Sciences 32:3-15.
- Markson, R. 1978. Solar modulation of atmospheric electrification and possible implications for the Sun-weather relationship. Nature 273:103-9.
- Mock, S. J., and W. D. Hibble III. 1975. Nature 261:484-6.
- Newman, T. G., and P. L. Odell. 1971. The generation of random variates. Number 21 of Griffin's statistical Monographs and Courses. Hafner Publishing Co. New York, New York.
- Olson, G. R. 1973. Range conditions on abandoned cropland in northcentral Montana. Missoula, University of Montana, unpublished M.S. thesis.
- Pearson, R. 1978. Climate and evolution. Academic Press. London.
- Roberts, W. O., and R. H. Olson. 1975. Nature 254:380
- Rowland F. S., and W. J. Molina. 1975. Chlorofluorocarbons in the environment. Review of Geophysics and Space Physics 13:1-36.

- Sandoval, F. M., and W. L. Gould. 1978. Improvement of saline- and sodium- affected disturbed lands, in Schaller, F. W., and P. Sutton eds., Reclamation of drastically disturbed lands. American Society of Agronomy, Crop Science Society of America, and Soil Science Society of America. Madison, Wisconsin, p.485-502.
- Schneider, S. H., and C. Mass. 1975. Volcanic dust, Sunspots and temperature trends. Science 190(4216):741-6.
- _____, and S. L. Thompson. 1979. Ice ages and orbital variations: some simple theory and modeling. Quaternary Research 12:188-203.
- Smit, J., and J. Hertogen. 1980. An extraterrestrial event at the Cretaceous-Tertiary boundary. Nature 285:198-200.
- Thorntwaite, C. W. 1931. The climates of North America according to a new classification. The geographical review 21:633-55.
- United States Department of Agriculture. 1975. Soil taxonomy -- A basic system of soil classification for making and interpreting soil surveys. Agricultural Handbook 436.
- United States Geological Survey, Department of the Interior and the Montana Department of State Lands. 1979. Draft Environmental statement, Regional analysis.
- Vines, R. G. 1977a. Fire and flood cycles- past and present. Presented at the symposium on environmental consequences of fire and fuel management in Mediterranean ecosystems, Palo Alto, California. August 1-5, 1977.
- _____, 1977b. Features of the Sun spot cycle. Presented at the symposium on environmental consequences of fire and fuel management in Mediterranean ecosystems, Palo Alto, California. August 1-5, 1977.
- Walsh, J. E., and A. Mostek. 1980. A quantitative analysis of meteorology anomaly patterns over the United States, 1900 - 1977. Monthly Weather review 108:615-30.
- Weertman, J. 1976. Milankovitch solar radiation variations and ice age sheet sizes. Nature 261:17-20.
- White, O. R. 1977. The Solar Output and its Variation. Colorado Associated University Press, Boulder, Colorado.
- Woillard, G. 1978. Grande Pile Peat Bog: A continuous pollen record for the last 140,000 years. Quaternary Research 9:1-21.

Appendix A

DERIVATION OF CONFIDENCE LIMITS FOR PI

The probability distribution of the estimated value of Pi based on the Monte-Carlo simulation will be worked out here to show that the method will converge to the correct answer at a rate proportional to the reciprocal of the square root of N.

Since the area of the unit circle divided by the area of the unit square is $\text{Pi}/4$, the expected number of hits (E_h) out of N tries is $N * \text{Pi}/4$, while the expected number of misses (E_m) is $N - E_h = N(4 - \text{Pi})/4$. The probability of observing any actual number of hits (O_h) out of N trials can be calculated via the Chi Square test. This test makes use of the following relationship:

$$\text{Chi Square} = \frac{(O_h - E_h)^2}{E_h} + \frac{(O_m - E_m)^2}{E_m}$$

Since O_h can be rewritten as $(E_h - x)$ and O_m can be rewritten as $(E_m + x)$, where x is the amount of deviation from the expected number of hits (E_h), or the expected number of misses (E_m), the deviation corresponding to any given probability level can be calculated by substituting $(E_h - x)$ for O_h and $(E_m + x)$ for O_m in the above equation and solving for x . This results in :

$$x = .25 * \sqrt{\text{Chi Square} * N * \text{Pi} * (4 - \text{Pi})}$$

This value of x can be used to calculate the distribution of results expected from the simulation. Since $Eh/N = \pi/4$, then $(Oh/N)*4$ is an approximation to π . Now $Oh = Eh \pm x$, so $[(Eh \pm x)/N]*4$ delimits the range of the approximation to π having a two-tailed significance level corresponding to the significance level of the chosen one-tailed Chi Square value. This approximation can be called W . Since $(\pi/4)*N = Eh$, then :

$$W = (4/N)*[(\pi*N/4) \pm x]$$

Rearranging this equation, and substituting for x , we obtain:

$$W = \pi \pm \sqrt{\frac{\text{Chi Square} * \pi * (4 - \pi)}{N}}$$

This demonstrates the convergence to π (at the rate of the square root of the reciprocal of N). This equation is used to plot the confidence limits to the approximation to π shown in Figure 14a.

Appendix B

TABLES OF RAW DATA

BILLINGS					
1905 - 1944					
INCHES OF PRECIPITATION					
YEAR	WINTER	SPRING	SUMMER	FALL	ANNUAL
1905		6.16	5.92	3.96	17.35
1906	0.73	6.78	4.12	1.92	13.94
1907	2.97	7.29	3.16	1.37	14.77
1908	2.83	7.65	3.09	3.92	17.37
1909	1.50	3.54	6.05	1.55	12.87
1910	0.99	3.04	2.44	4.14	11.28
1911	2.63	4.32	3.38	1.49	10.94
1912	0.87	4.87	5.08	7.11	17.65
1913	0.55	2.58	4.84	4.64	12.74
1914	0.68	3.58	5.41	2.14	11.88
1915	1.05	4.25	9.21	3.60	18.55
1916	1.75	4.51	6.47	3.50	16.07
1917	1.34	6.67	3.45	2.54	15.05
1918	4.24	4.63	3.76	4.08	15.21
1919	0.26	1.83	1.70	4.42	8.93
1920	2.31	4.82	3.16	0.51	10.45
1921	0.52	5.01	3.73	1.84	11.15
1922	2.07	5.04	4.97	2.72	14.67
1923	0.87	4.83	7.18	6.85	19.71
1924	1.05	4.56	3.83	1.96	11.89
1925	1.71	3.83	5.33	3.18	14.55
1926	1.92	2.50	2.07	3.74	9.47
1927	1.60	6.14	6.65	2.62	17.52
1928	2.96	1.41	4.94	3.16	12.01
1929	2.07	2.82	2.25	3.59	10.75
1930	1.70	1.84	3.36	3.04	9.30
1931	0.44	2.27	1.98	3.60	8.35
1932	1.14	6.05	6.41	3.79	18.40
1933	2.86	4.53	4.66	1.44	13.24
1934	1.30	2.20	3.98	1.79	8.74
1935	0.70	5.52	3.21	1.42	11.26
1936	2.19	2.03	3.28	2.30	9.35
1937	1.27	2.06	5.42	5.77	14.83
1938	0.97	7.05	6.51	4.02	18.05
1939	0.90	3.71	8.10	1.28	14.07
1940	2.25	9.91	3.60	5.26	20.99
1941	0.37	8.24	5.63	8.19	23.26
1942	1.87	8.49	4.02	4.34	17.97
1943	1.65	2.75	5.51	1.85	11.61
1944	1.19	1.65	12.80	3.04	19.91

BILLINGS
1945 - 1979
INCHES OF PRECIPITATION

YEAR	WINTER	SPRING	SUMMER	FALL	ANNUAL
1945	2.16	3.52	5.21	3.17	13.57
1946	1.39	2.32	4.54	5.38	13.68
1947	1.80	3.53	5.26	3.35	14.00
1948	1.54	2.68	3.37	0.71	8.11
1949	2.68	2.82	3.89	4.71	14.09
1950	1.74	3.35	4.74	3.12	12.90
1951	1.76	3.00	4.63	2.28	11.55
1952	1.24	4.71	2.97	1.17	9.66
1953	1.00	3.31	5.32	2.61	12.18
1954	0.57	3.68	2.43	1.31	8.28
1955	1.50	7.70	3.24	2.34	15.57
1956	1.73	3.09	2.88	2.20	9.11
1957	0.98	9.22	7.23	3.87	20.96
1958	1.40	2.87	5.98	1.81	12.92
1959	2.02	3.33	1.98	3.16	10.07
1960	1.20	2.25	2.73	1.22	7.34
1961	0.70	4.20	1.33	6.34	12.29
1962	2.21	4.55	4.94	1.89	13.52
1963	1.92	4.90	3.63	2.24	13.66
1964	1.33	9.57	8.65	0.79	19.64
1965	1.67	3.65	7.18	2.90	15.51
1966	0.94	2.77	4.48	2.97	11.26
1967	1.23	3.82	6.89	2.10	14.16
1968	2.19	3.56	7.04	3.30	16.02
1969	1.61	2.64	8.16	2.22	14.27
1970	1.69	7.36	2.96	4.03	16.12
1971	1.67	4.11	2.22	5.74	14.08
1972	3.47	3.77	4.55	4.68	16.53
1973	1.57	5.55	2.66	4.23	14.85
1974	2.26	4.94	5.08	5.85	16.76
1975	2.21	5.02	4.70	3.94	16.76
1976	1.99	6.21	3.60	2.68	13.69
1977	1.41	2.68	1.13	2.57	8.89
1978	4.59	10.96	3.21	6.59	24.70
1979	2.01	1.94	2.24	1.68	7.22
AVERAGE	1.64	4.46	4.56	3.21	13.87
STD. DEV.	0.82	2.14	2.04	1.62	3.77

BUSBY					
1911 - 1944					
INCHES OF PRECIPITATION					
YEAR	WINTER	SPRING	SUMMER	FALL	ANNUAL
1911		3.15	5.43	2.75	12.75
1912	1.86	6.84	8.28	5.62	21.98
1913	1.18	4.89	4.51	3.81	14.38
1914	0.67	4.54	6.66	2.43	14.39
1915	1.39	3.37	11.12	3.12	19.18
1916	2.34	3.63	2.87	2.53	11.43
1917	1.05	4.57	2.15	0.68	9.65
1918	3.73	4.90	6.55	4.37	18.37
1919	0.77	1.77	3.00	3.42	9.07
1920	1.68	5.12	5.73	1.43	13.73
1921	0.61	2.93	2.25	2.16	8.07
1922	1.57	4.46	4.46	1.85	12.90
1923	1.30	3.82	4.20	7.62	16.18
1924	1.79	4.68	2.46	3.50	13.08
1925	1.90	5.28	4.21	2.76	14.10
1926	2.03	2.88	6.17	3.43	14.09
1927	1.40	6.47	7.17	2.53	17.95
1928	3.29	1.72	7.42	2.25	14.19
1929	1.37	2.32	2.39	3.60	9.61
1930	0.83	2.36	3.62	2.29	8.97
1931	0.90	1.00	2.63	4.19	8.74
1932	0.60	3.57	4.30	3.09	11.92
1933	1.17	5.06	5.48	1.89	13.77
1934	1.16	0.91	1.37	2.87	5.97
1935	0.60	3.74	5.68	1.77	11.60
1936	0.93	1.80	1.82	2.19	6.78
1937	0.88	1.79	5.25	2.81	11.16
1938	1.24	5.07	3.68	1.53	11.05
1939	0.65	3.89	4.28	1.29	10.29
1940	0.98	3.52	4.28	2.62	11.38
1941	0.44	3.23	5.17	3.91	13.67
1942	1.55	4.46	6.68	4.66	16.44
1943	1.55	2.92	5.17	2.42	11.95
1944	0.85	4.90	10.47	0.83	17.57

BUSBY
1945 - 1979
INCHES OF PRECIPITATION

YEAR	WINTER	SPRING	SUMMER	FALL	ANNUAL
1945	1.69	5.74	4.65	3.02	14.74
1946	1.08	4.19	4.78	5.43	15.77
1947	0.94	3.40	4.78	1.96	10.99
1948	1.44	3.92	6.24	1.60	12.79
1949	1.50	3.38	2.35	2.72	10.29
1950	0.88	3.66	5.52	2.31	12.26
1951	1.30	3.82	6.67	3.07	15.04
1952	0.98	2.16	3.13	0.93	6.96
1953	1.51	5.60	3.17	2.84	13.03
1954	1.04	2.85	3.21	2.18	9.14
1955	0.57	8.85	4.10	1.94	16.46
1956	1.27	4.28	5.53	2.55	12.87
1957	1.53	5.77	4.00	2.58	13.65
1958	0.56	2.43	9.09	2.99	15.99
1959	2.00	4.12	1.66	3.39	10.36
1960	0.80	2.90	3.90	0.86	10.01
1961	2.49	3.09	2.27	5.57	12.31
1962	2.64	4.52	7.70	2.11	17.01
1963	2.98	4.23	4.35	2.19	13.93
1964	1.79	4.91	8.33	0.82	15.29
1965	2.19	2.48	2.95	2.97	10.86
1966	1.53	3.40	4.88	3.44	13.50
1967	2.41	3.64	6.91	5.59	18.92
1968	2.88	4.49	9.96	3.47	20.53
1969	2.33	4.13	7.58	2.04	16.72
1970	3.58	9.42	3.46	4.81	21.10
1971	5.18	4.22	2.52	5.36	16.64
1972	2.83	4.53	4.94	2.97	15.10
1973	1.59	4.04	4.94	4.38	14.94
1974	1.64	5.87	5.63	4.97	17.92
1975	2.32	6.40	4.54	3.79	17.65
1976	2.09	4.35	5.31	2.67	13.87
1977	2.00	5.01	3.69	3.82	15.25
1978	2.61	10.44	2.53	5.40	20.71
1979	1.82	3.51	4.27	1.28	10.23
AVERAGE	1.62	4.14	4.88	3.04	13.61
STD. DEV.	0.88	1.72	2.13	1.28	3.56

CROW AGENCY 1900 - 1944					
INCHES OF PRECIPITATION					
YEAR	WINTER	SPRING	SUMMER	FALL	ANNUAL
1900		4.60	2.98	2.51	10.90
1901	0.57	4.64	2.91	2.47	11.09
1902	1.53	6.00	2.95	0.80	11.30
1903	2.43	3.45	6.06	3.15	15.68
1904	4.32	3.81	3.60	2.05	13.78
1905	2.91	6.27	6.61	4.34	18.83
1906	1.36	6.53	5.96	2.60	17.40
1907	2.82	8.34	6.01	2.30	19.28
1908	2.23	8.67	4.40	4.50	19.89
1909	2.11	5.58	3.55	3.32	15.86
1910	3.62	4.48	3.57	5.20	15.73
1911	3.23	3.55	4.03	3.17	14.41
1912	2.61	7.46	9.37	7.20	25.27
1913	1.63	3.28	3.57	4.98	13.40
1914	0.88	4.98	3.29	2.63	12.08
1915	1.78	5.11	4.49	3.65	15.47
1916	2.23	5.11	4.49	3.65	15.47
1917	2.23	5.11	3.64	2.33	14.00
1918	4.15	2.30	4.93	5.59	15.52
1919	0.45	2.16	2.64	3.65	9.54
1920	4.05	5.96	5.63	2.03	17.75
1921	2.24	9.11	2.36	1.55	14.67
1922	2.28	4.05	5.70	2.60	15.95
1923	2.16	5.16	7.45	8.59	22.59
1924	2.45	6.00	5.43	2.47	17.23
1925	3.91	4.15	1.66	5.30	15.13
1926	3.79	2.37	4.91	6.50	16.46
1927	1.45	10.60	7.63	5.39	26.21
1928	5.70	3.47	4.17	5.34	17.68
1929	2.35	3.52	2.15	5.21	12.68
1930	1.11	3.95	3.11	3.22	11.43
1931	1.35	2.26	4.22	5.61	14.06
1932	2.53	7.28	3.60	7.12	20.65
1933	2.95	8.22	1.55	1.72	15.46
1934	2.50	2.92	1.70	2.80	8.78
1935	1.53	7.20	4.23	2.64	15.54
1936	3.33	2.66	2.59	2.77	11.41
1937	2.94	2.17	2.37	3.10	10.63
1938	1.22	7.25	6.97	1.84	16.46
1939	1.41	5.58	5.03	1.35	13.97
1940	2.46	6.15	4.56	2.38	15.31
1941	0.54	5.09	4.71	8.18	19.41
1942	2.02	5.61	3.47	4.73	15.39
1943	2.67	3.30	7.28	3.35	15.82
1944	1.02	3.51	10.39	1.98	17.92

CROW AGENCY
1945 - 1979
INCHES OF PRECIPITATION

YEAR	WINTER	SPRING	SUMMER	FALL	ANNUAL
1945	2.31	5.44	5.11	3.09	15.98
1946	2.45	4.44	5.05	7.57	19.48
1947	1.84	4.78	4.85	3.26	14.24
1948	1.97	5.70	6.18	1.05	14.67
1949	2.82	3.86	1.82	2.79	11.99
1950	1.81	5.05	6.83	3.18	16.75
1951	2.27	3.23	5.00	3.33	14.08
1952	2.09	2.61	4.26	1.08	8.93
1953	1.63	4.57	3.16	4.06	13.51
1954	1.33	4.16	2.50	2.01	10.09
1955	1.51	10.93	2.70	2.85	18.84
1956	1.43	3.05	4.15	2.44	10.29
1957	1.43	9.54	7.26	3.29	21.20
1958	0.95	1.62	6.11	3.58	13.51
1959	2.54	3.82	1.47	3.68	10.59
1960	1.31	2.80	2.19	1.12	8.45
1961	2.19	3.54	1.97	7.80	14.40
1962	1.84	3.37	4.05	3.04	12.30
1963	1.91	4.46	3.85	2.01	12.88
1964	1.61	8.51	8.63	1.35	19.47
1965	2.05	4.49	5.81	2.88	15.71
1966	2.18	3.29	2.77	3.06	11.24
1967	2.22	4.23	3.75	4.70	15.17
1968	2.98	6.23	7.84	3.91	21.02
1969	1.71	6.01	6.12	2.53	16.21
1970	2.93	9.34	1.47	4.17	17.60
1971	4.15	4.17	3.87	5.69	18.08
1972	2.55	3.59	5.66	4.33	16.17
1973	1.30	7.17	4.60	4.94	18.31
1974	2.41	6.94	6.14	5.65	20.53
1975	3.67	8.51	4.13	4.28	21.09
1976	2.01	4.81	4.32	4.06	14.54
1977	1.66	5.90	3.73	5.58	17.85
1978	4.02	10.73	2.69	8.95	26.04
1979	2.33	3.93	2.29	1.42	9.28
AVERAGE	2.26	5.17	4.43	3.75	15.55
STD. DEV.	0.97	2.17	1.90	1.77	3.86

MILES CITY					
1900 - 1944					
INCHES OF PRECIPITATION					
YEAR	WINTER	SPRING	SUMMER	FALL	ANNUAL
1900		3.85	7.99	2.51	15.01
1901	0.67	2.58	8.71	2.70	15.22
1902	1.04	5.18	4.70	0.68	11.16
1903	0.94	1.93	5.09	2.18	10.05
1904	0.91	4.50	3.47	0.32	9.20
1905	0.58	2.11	7.03	2.82	12.49
1906	0.88	6.03	6.53	1.97	16.71
1907	3.02	5.88	6.57	0.45	14.85
1908	1.63	8.32	5.42	2.37	17.67
1909	1.50	3.63	4.54	2.43	12.23
1910	2.14	4.25	4.03	3.55	14.01
1911	2.15	1.30	6.41	3.49	14.46
1912	2.78	8.31	6.31	4.44	20.41
1913	2.17	4.82	6.30	4.84	18.06
1914	1.52	2.07	6.77	3.31	14.15
1915	2.88	1.71	12.59	3.45	21.03
1916	2.49	2.52	8.09	2.32	16.53
1917	3.59	4.00	3.20	1.26	12.55
1918	4.33	3.91	3.90	2.43	12.71
1919	1.51	3.42	1.99	4.51	11.33
1920	1.98	2.86	6.07	1.15	12.20
1921	1.40	3.53	8.88	3.45	17.92
1922	3.22	7.44	4.24	1.68	16.04
1923	1.38	3.61	4.91	7.68	17.08
1924	1.59	2.75	2.84	1.64	9.58
1925	2.05	3.16	4.87	2.44	12.18
1926	2.06	1.92	3.83	2.34	10.08
1927	1.53	7.37	5.60	3.52	18.71
1928	2.19	1.52	7.85	1.98	12.62
1929	1.73	4.74	3.98	3.53	14.13
1930	1.31	3.55	3.88	2.17	10.68
1931	0.88	1.43	2.37	1.49	6.41
1932	1.72	5.11	5.80	2.69	15.31
1933	2.12	3.62	2.75	1.76	10.52
1934	1.04	1.89	1.89	1.53	5.91
1935	0.87	3.60	5.61	1.32	11.80
1936	1.85	1.64	1.62	1.66	6.37
1937	1.04	2.35	5.18	2.11	10.75
1938	1.09	3.95	4.88	1.74	11.56
1939	1.07	2.60	5.68	0.77	10.15
1940	1.18	4.71	5.24	3.29	14.42
1941	0.74	3.90	7.23	6.03	18.07
1942	1.38	4.46	6.94	1.90	14.27
1943	1.20	2.02	9.81	2.57	15.50
1944	1.05	4.08	12.53	1.30	19.17

MILES CITY
1945 - 1979
INCHES OF PRECIPITATION

YEAR	WINTER	SPRING	SUMMER	FALL	ANNUAL
1945	0.84	4.51	4.85	2.62	12.93
1946	0.67	4.51	4.47	8.28	18.12
1947	1.19	3.70	6.49	1.11	12.23
1948	1.55	3.55	10.24	1.01	16.39
1949	2.49	2.15	2.00	2.71	9.37
1950	1.35	3.97	4.76	2.84	12.97
1951	0.88	2.00	7.41	2.54	13.58
1952	2.21	2.37	3.44	1.17	8.12
1953	1.64	7.04	6.41	2.21	17.44
1954	0.98	2.79	5.52	2.23	11.35
1955	1.19	7.27	2.99	1.74	13.59
1956	1.07	2.97	5.43	1.83	11.09
1957	1.27	5.18	5.55	2.36	14.14
1958	1.04	2.27	5.90	2.81	12.54
1959	2.59	2.86	2.91	2.83	10.70
1960	0.86	3.05	2.45	0.64	7.49
1961	1.49	3.92	3.17	3.76	12.02
1962	0.97	6.03	7.60	2.40	17.09
1963	1.93	4.46	6.52	2.17	15.13
1964	1.44	3.05	7.42	1.45	13.62
1965	1.87	3.92	6.51	2.51	14.56
1966	1.50	2.34	5.98	1.58	11.38
1967	1.50	5.59	7.20	3.52	18.47
1968	2.15	2.97	10.17	1.38	16.57
1969	1.43	4.66	5.55	0.93	12.51
1970	1.44	4.66	3.22	2.42	11.20
1971	1.77	2.08	3.83	6.63	14.52
1972	1.38	3.28	8.63	1.08	14.48
1973	0.96	5.43	5.23	4.70	16.23
1974	0.80	4.80	3.25	2.56	11.10
1975	1.03	4.90	4.63	3.05	13.83
1976	0.71	2.56	5.76	2.24	11.12
1977	1.00	3.46	5.32	3.34	13.65
1978	1.59	6.78	4.72	5.31	18.01
1979	1.36	2.00	3.95	1.07	8.00
AVERAGE	1.55	3.82	5.54	2.61	13.46
STD. DEV.	0.71	1.64	2.25	1.41	3.30

AVERAGE MONTHLY PRECIPITATION

MONTH	BILLINGS 1905 - 1979		BUSBY 1911 - 1979	
	AVERAGE	STD. DEV.	AVERAGE	STD. DEV.
January	0.62	0.46	0.63	0.51
February	0.47	0.36	0.44	0.29
March	0.73	0.44	0.62	0.34
April	1.41	1.14	1.31	0.81
May	2.32	1.43	2.21	1.31
June	2.46	1.79	2.50	1.34
July	1.06	0.76	1.29	0.94
August	1.04	0.83	1.09	1.00
September	1.37	1.11	1.32	1.12
October	1.19	0.93	1.05	0.72
November	0.65	0.46	0.61	0.43
December	0.55	0.39	0.54	0.39
ANNUAL	13.87	3.77	13.61	3.56

MONTH	CROW AGENCY 1900 - 1979		MILES CITY 1900 - 1979	
	AVERAGE	STD. DEV.	AVERAGE	STD. DEV.
January	0.78	0.56	0.55	0.38
February	0.70	0.44	0.45	0.27
March	1.09	0.76	0.71	0.51
April	1.74	1.22	1.12	0.77
May	2.34	1.45	1.98	1.28
June	2.43	1.46	2.75	1.60
July	1.05	0.86	1.58	1.13
August	0.95	0.82	1.21	0.96
September	1.53	1.33	1.15	1.02
October	1.31	1.00	0.87	0.92
November	0.87	0.63	0.54	0.43
December	0.75	0.49	0.54	0.43
ANNUAL	15.55	3.86	13.46	3.30

Appendix C

GENERATION AND TESTING OF RANDOM DEVIATES

The generation of random deviates

Due to the important role that random numbers play in the determination of various critical values in this paper, extensive work went into the generation and testing of random numbers.

The final method chosen was a compound linear congruential generator. In this method, a sequence of pseudo-random numbers uniformly distributed between 0 and 1 is obtained via the following formula:

$$X_{n+1} = ((A_1 * X_n + C_1) \text{MODULUS } M_1) / M_1$$

These values are stored in an array of length 4567. A second uniform random sequence is obtained in the same manner that the first sequence was generated. i.e.:

$$Y_{n+1} = ((A_2 * Y_n + C_2) \text{MODULUS } M_2) / M_2$$

These random numbers are scaled between 1 and 4567 and are used as the address of the array from which random numbers are picked. A new X is then generated as above and placed in the array location held by the random number finally chosen. The chosen random number is then also scaled between 1 and 4567 and is used as the address of the array whose value is interchanged with another location whose address is found via a third linear congruential generator, i.e.:

$$Z_{n+1} = 1 + \left(\left(\frac{A * Z_n + C}{M} \right) \text{MODULUS } M \right) * 4567$$

This last operation has the effect of partially shuffling the array each time a random number is generated. The values of A, C, and M (the multiplier, increment and modulus base respectively) were chosen in accord with the following recommendations of Kneuth (1969).

- i) The starting number of the series may be chosen arbitrarily. If the program is to be run several times and a different source of random numbers is desired each time, change the starting value each time.
- ii) The number M should be large. It may conveniently be taken as the computer's word size, since this makes the computation of the random number quite efficient. The computations must be done without any roundoff error.
- iii) If M is a power of 2, choose A so that $(A) \text{Modulus } 200 = 21$. This choice of A together with the choice of C given below will ensure that the random number generator will produce all M different possible values of X before it starts to repeat and ensures high potency.
- iv) The multiplier A should be larger than M, preferable larger than $M/100$, but smaller than $M\text{-Square Root}(M)$. The digits in the binary or decimal representation of A should not have a simple, regular pattern. The best policy is to take some haphazard constant to be the multiplier, such as 3141592621.
- v) The constant C should be an odd number when M is a power of 2 and also not a multiple of 5 when M is a power of 10. It is preferable to choose C so that C/M has approximately the value of $(1/6) * (3\text{-Square Root}(3))$; (i.e. = .21132).
- vi) The least significant digits of X are not very random, so decisions based on the numbers should always be primarily influenced by the most significant digits. It is generally best to think of X as a random fraction between 0 and 1 rather than as a random integer between 0 and M-1.

Accordingly, the following values were used to generate the three random series used in this paper (X, Y, and Z):

SERIES	A	C	M
X	30517577984	7261067087	34359738368
Y	314159221	2718281829	34359738368
Z	61681	628521	909091

A FORTRAN program to carry out this scheme is presented in this appendix. As indicated above, the values generated by this method are uniformly distributed between 0 and 1. They are then converted into standard deviates via the method proposed by Box and Muller (1958). The method can be summarized as follows.

Let U and V be independent random variables, both uniformly distributed between 0 and 1. If:

$$X = \sqrt{-2 * \text{Natural logarithm of } U} * \text{Cosine}(2\text{Pi} * V)$$

and

$$Y = \sqrt{-2 * \text{Natural logarithm of } U} * \text{Sine}(2\text{Pi} * V)$$

Then X and Y will be independent random variables, normally distributed with mean 0 and variance 1.

FORTTRAN subroutine to produce random numbers

```

SUBROUTINE RANDU(RAN)
IMPLICIT DOUBLE PRECISION (D)
COMMON/RAN/XARR(4567),IX,IY,XZ,ISW
DATA IX/1319/
DATA XZ/628521.0/
DATA DC3/192113.0D+00/
DATA DA3/61681.0D+00/
DATA DM3/909091.0D+00/
DATA IY/133921/
DATA IA2/3141592221/
DATA DC2/2718281829.0D+00/
DATA IA/30517578125/
DATA ISW/1/
DATA DC/7261067087.0D+00/
DATA DTEMP/0.291038304567337036D-10/
GOTO (1,3)ISW
1 DO 2 I=1,4567
    IX=IX*IA
    IX=IX+DC
2 XARR(I)=IX*DTEMP
  ISW=2
3 IY=IY*IA2
  IY=IY+DC2
  INXT=((IY*DTEMP)*4567.0)+1
  RAN=XARR(INXT)
  IX=IX*IA
  IX=IX+DC
  XARR(INXT)=IX*DTEMP
  INDEX=(RAN*4567)+1
  XZ=DMOD(((XZ*DA3)+DC3),DM3)
  INDEX3=((XZ/DM3)*4567)+1
  TEMP=XARR(INDEX)
  XARR(INDEX)=XARR(INDEX3)
  XARR(INDEX3)=TEMP
RETURN
END

```

The testing of Randu's random numbers

In order to test both the local and global behavior of the random numbers used in this study, 4000 series, each of 250 random numbers, were constructed using the subroutine RANDU listed in this appendix. The following tests were applied to each series and the results of each test tabulated.

1) The Cramer-von Mises goodness of fit test

Test statistic = T where:

$$T = \frac{1}{12*N} + \sum_{i=1}^N [F(x_i) - \frac{2i-1}{2*N}]^2$$

$F(x_i)$ = The hypothesised distribution function

Distribution of T:

Probability Level	Critical Value	Probability Level	Critical Value
.10	.046	.90	.347
.30	.079	.95	.461
.50	.119	.99	.743
.70	.184	.999	1.168

2) The Kolmogorov goodness of fit test

Test statistic = T where:

$$T = \sup_x |F(x_i) - S(x_i)|$$

$F(x_i)$ = The hypothesised distribution function

$S(x_i)$ = The empirical distribution function

\sup_x = The largest value of $|F(x_i) - S(x_i)|$ observed

Distribution of T:

$$W(\alpha) = \text{SQRT}(-\ln(\alpha/2)/(2*N))$$

3) The Chi-Square test for uniform distribution

Test statistic = Chi-Square where:

$$\text{Chi Square} = \sum_{i=1}^c \frac{(O_i - E_i)^2}{E_i}$$

O_i = The observed number of variates in class i

E_i = The expected number of variates in class i

c = The number of classes

Distribution of Chi Square:

The Chi Square distribution with
($c-1$) degrees of freedom

4) Wald-Wolfowitz number of runs test

Test statistic = T where:

T = Number of runs of like elements in the series

Distribution of T

$$W(\alpha) = \frac{2MN}{M+N} + 1 + X \frac{\sqrt{2MN(2MN-M-N)}}{(M+N)*(M+N)*(M+N-1)}$$

Where:

M = The number of element type 1 in the series

N = The number of element type 2 in the series

X = The normal deviate corresponding to
the alpha probability level

5) Wallis - More length of runs test

Test statistic = Chi Square where:

$$\text{Chi Square} = \sum_{i=1}^L \frac{(O_i - E_i)^2}{E_i}$$

O_i = Observed number of runs
of length i in series

E_i = Expected number of runs
of length i in series

Distribution of test statistic

Chi Square distribution with
($L-1$) degrees of freedom

6) $R \times C$ contingency table test for independence of successive values

Test statistic = T , where:

$$T = \sum_{i=1}^R \left[\sum_{j=1}^C \frac{(O_{ij} - E_{ij})^2}{E_{ij}} \right]$$

R = Number of rows in the table

C = The number of columns in the table

O_{ij} = Observed number of variates in cell ij

E_{ij} = Expected number of variates in cell ij

Distribution of test statistic:

Chi Square distribution with
($R-1$)*($C-1$) degrees of freedom

7) Minimum and Maximum of N test

Test statistics = T_{min} and T_{max}

$$T_{min} = (1.0 - \text{Minimum of } N \text{ successive values})^N$$

$$T_{max} = (\text{Maximum of } N \text{ successive values})^N$$

Distribution of test statistics

Both T_{max} and T_{min} are uniformly
distributed between 0 and 1

The resulting distributions of test statistics from each series of

tests were compared against the expected distribution of test statistics using the Chi Square test. The random number generator used in this study passed all these tests and therefore was considered a source of uniformly distributed random numbers.

The first 100 random numbers produced by Randu

(1)	(2)	(3)	(4)	(5)	
.9258	.8525	.1647	.5689	.7717	
.3071	.5888	.4977	.6295	.6871	(10)
.5183	.7746	.9315	.3533	.8201	
.6599	.6326	.9136	.5343	.4926	(20)
.9005	.3753	.8397	.4167	.6793	
.4078	.9726	.1764	.9503	.2015	(30)
.2586	.0157	.7181	.5773	.2203	
.6761	.6975	.7470	.3658	.8984	(40)
.6432	.1112	.7862	.9910	.8409	
.4235	.7899	.8941	.9800	.2688	(50)
.2054	.1124	.3301	.4838	.5876	
.0565	.3342	.3524	.6821	.5387	(60)
.5673	.9286	.0363	.8204	.7554	
.8927	.5605	.9548	.7352	.5299	(70)
.6586	.1466	.5750	.3169	.7242	
.2554	.5585	.2739	.0519	.4033	(80)
.2791	.8682	.7847	.1455	.1151	
.9951	.0872	.5760	.8157	.4824	(90)
.0034	.1297	.7158	.4303	.3785	
.2358	.1640	.9278	.5031	.8904	(100)

Appendix D

FORTRAN SUBROUTINE TO CALCULATE THE FOURIER TRANSFORM

```

SUBROUTINE FFT(N,X,AMP,ARG)
DIMENSION X(1),AMP(1),ARG(1)
C  N    = NUMBER OF POINTS OF THE REAL ARRAY X
C  AMP  = ARRAY OF AMPLITUDES FROM 0 TO N/2
C  ARG  = ARRAY OF PHASES FROM 0 TO N/2
NE=(ALOG(N)/ALOG(2))-1
CALL RECOOL(NE,X)
DO 1 I=1,N/2
    JJ=2*I
    J=JJ-1
    AMP(I)=SQRT((X(J)*X(J))+(X(JJ)*X(JJ)))
1   ARG(I)=ATAN2(X(JJ),X(J))
RETURN
END

```

```

SUBROUTINE RECOOL(N,X)
DIMENSION X(1),G(2)
COMPLEX X,A,B,W,CONJG
EQUIVALENCE(G,W)
L=2**N
CALL COOL(N,X,-1.)
ARG=3.14159265/L
G(1)=COS(ARG)
G(2)=SIN(ARG)
B=CONJG(X(1))
A=X(1)
X(1)=(A+B+(0.,1.)*(B-A))*0.5
X(L+1)=(A+B-(0.,1.)*(B-A))*0.5
LL=L/2+1
DO 1 I=2,LL
    J=L-I+2
    B=CONJG(X(I))
    A=B+X(J)
    B=(X(J)-B)*W**(I-1)
    X(J)=(A+(0.,1.)*B)*0.5
1 X(I)=(CONJG(A)+(0.,1.)*CONJG(B))*0.5
RETURN
END

```

```

COMPLEX FUNCTION CONJG(Z)
DIMENSION Z(2)
CONJG=Z(1)-(0.,1.)*Z(2)
RETURN
END

```

```

SUBROUTINE COOL(N,X,SIGNI)
COMPLEX X,Q,W,HOLD
DIMENSION X(2048),INT(16),G(2)
EQUIVALENCE (G,W)
LX=2**N
FLX=LX
IL=LX
FLXPI2=SIGNI*6.2831853/FLX
DO 1 I=1,N
  IL=IL/2
1 INT(I)=IL
NBLOKK=1
DO 4 LAYER=1,N
  NBLOCK=NBLOKK
  NBLOKK=NBLOKK+NBLOKK
  LBLOCK=LX/NBLOCK
  LBHALF=LBLOCK/2
  NW=0
  DO 4 IBLOCK=1,NBLOCK
    LSTART=LBLOCK*(IBLOCK-1)
    FNW=NW
    ARG=FNW*FLXPI2
    G(1)=COS(ARG)
    G(2)=SIN(ARG)
    DO 2 I=1,LBHALF
      J=I+LSTART
      K=J+LBHALF
      Q=X(K)*W
      X(K)=X(J)-Q
2    X(J)=X(J)+Q
      DO 3 I=2,N
        LL=(NW.AND.INT(I))
        IF(LL)3,4,3
3      NW=NW-INT(I)
4    NW=NW+INT(I)
    NW=0
    DO 8 K=1,LX
      NW1=NW+1
      IF(NW1-K)6,6,5
5      HOLD=X(NW1)
      X(NW1)=X(K)
      X(K)=HOLD
6      DO 7 I=1,N
        LL=(NW.AND.INT(I))
        IF(LL)7,8,7
7      NW=NW-INT(I)
8    NW=NW+INT(I)
  RETURN
END

```